A 2.45 GHz Frequency-Selective Rectenna for Wireless Energy Harvesting

by

Reza Ashtari

A dissertation submitted to the Graduate Faculty of
Auburn University
in partial fulfillment of the
requirements for the Degree of
Doctor of Philosophy

Auburn, Alabama
August 6, 2016

Keywords: energy harvesting, frequency selective surface, rectenna

Approved by

Michael Baginski, Chair, Associate Professor of Electrical and Computer Engineering
Robert Dean, Associate Professor of Electrical and Computer Engineering
Lloyd Riggs, Professor of Electrical and Computer Engineering
Thaddeus Roppel, Associate Professor of Electrical and Computer Engineering

Abstract

As the emphasis placed on renewable energies has grown over recent years, a necessity for innovative methods of providing alternative energy sources has emerged. With most modern communication systems utilizing radio transmissions, significant amounts of broadcasted radio emissions are regularly wasted. Implementing radio energy scavenging systems in such areas provides an opportunity to save otherwise wasted energy in these environments. Providing a novel wireless energy scavenging system, this paper presents a linearly polarized rectenna using a two diode system for the rectification circuit. The rectenna uses a dipole square patch antenna with a frequency-selective surface (FSS), which behaves as a filter while also reducing the size of the rectenna. Made using multiple layers, the rectenna consists of two Rogers 5880 Duroid substrates 508 μm (20 mil) in thickness with an effective permittivity of 2.2 and a Rohacell foam spacer 5 mm in thickness with an effective permittivity of 1. This dual-diode FSS rectenna reaches a RF-to-DC conversion efficiency of 79% at 2.45 GHz. The use of a FSS replaces the traditional transmission line filter used in most rectenna systems while improving the matching of the antenna and reducing the surface area of the rectenna. The rectenna is linearly polarized with a broad angle of energy reception for absorption of ambient radio waves within the ISM band and is well-suited for energy harvesting applications.

Acknowledgments

I would like to thank Dr. Michael Baginski for his assistance and guidance throughout the development of this research as well as Dr. Shiwen Mao for their continued support throughout my undergraduate and graduate career.

I would also like to thank Lloyd Riggs for allowing me to use his equipment for my research and Joe Haggerty for his help with the fabrication of the materials used for this project and also my committee members for their cooperation and time in seeing my PhD through.

If it wasn't for the opportunities you all helped me make the most of, I would not have ever had the privilege of pursuing my research interests and reaching where I am today.

Table of Contents

List of Figures

List of Tables

Chapter 1

Introduction

Presently there is an ever increasing interest in developing alternative sources of accessible energy. Solar, hydroelectric, and wind are all regularly used for powering devices ranging from streetlights to satellites. However, the amount of semi-ambient, man-made microwave power available in many urban environments is also an excellent source of free energy that would otherwise be wasted. The focus of the research presented here is on developing a very efficient microwave energy scavenging system applicable to urban environments.

Typical microwave energy harvesting technologies convert microwave energy to power supply level DC voltages that power nearby systems. The conversion from microwave energy to DC voltage (V) normally occurs via the use of rectifier circuitry and an antenna or "rectenna". Rectennas capture high frequency microwave energy at the antenna level and convert the energy to a high frequency voltage that must be impedance matched to the rectifier circuit resulting in steady DC voltage.

The maximum amount of energy scavenged by the antenna is proportional to the effective aperture of the antenna and therefore, the overall antenna aperture becomes the critical factor that determines rectenna performance. The matching and rectification networks are designed to maximize the AC-DC conversion efficiency and available DC voltage and power. Rectification circuitry typically consists of a series of short transmission line segments and RF diodes that convert the AC signal to DC at the load impedance.

Many current state-of-the-art microwave energy scavenging systems utilize patch antennas typically operating in the microwave band from 1 - 8 GHz (Donchev et al., 2014). Patch antennas are conformal to planar surfaces and have a relatively small form factor for their respective aperture. They are also easily fabricated and the necessary impedance matching

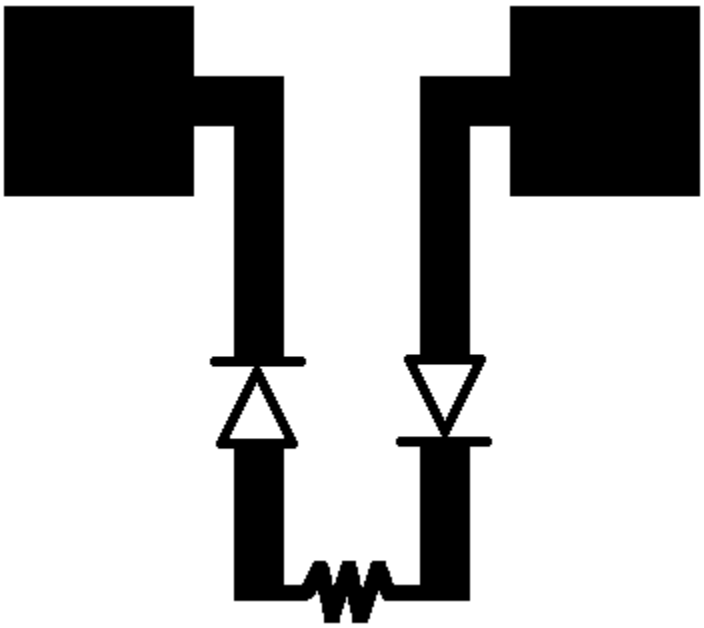

Figure 1.1: Rectenna diagram. Antenna, rectification circuit, and load resistance are depicted in black. Frequency selective surface is depicted in gray.

networks and filters are placed in the adjacent space to create compact designs (Ren and Chang, 2006), (Hong et al., 2010), (Lee and Chang, 2015).

The antenna on the front-end of a rectenna system converts incident radio waves to alternating current (AC) electrical signals. The matching and filtering networks of the rectenna serve to eliminate unwanted energy received from the antenna. This is crucial to the RF-to-DC conversion efficiency of the rectenna as such systems are designed to operate within a specified frequency range and energy outside of this designed range will otherwise be wasted. The rectification circuit, comprised of a series of transmission lines and RF diodes, convert the matched AC signal to DC. Finally, the rectenna system terminates in a load resistance, across which the output DC voltage is measured.

The rectenna presented in this paper is designed specifically for wireless energy harvesting and therefore the antenna used is adapted to better serve this application.

Wireless scavenging systems take advantage of linear polarization as ambient and scattered radio energy is typically linear in nature.

The antenna is designed for omnidirectionality to better receive radio energy within a wireless harvesting application where the direction of incident radio waves is unknown. Again, this is the opposite from what would be seen in a line-of-sight wireless power transmission system where a highly directional antenna would be preferred.

For matching, rectenna systems typically use transmission line filters such as stub matching networks or tee resonators. These approaches are somewhat effective; however ultimately perform the filtering at the expense of much surface area. Thus using stub matching networks to minimize return loss is not a practical method for yielding a size-sensitive rectenna.

Proving to be a superior alternative to typical stub-matched systems, a frequency selective surface (FSS) was used. The FSS took the place of a traditional ground plane, significantly reducing the surface area otherwise occupied via the use of a stub matching system. In addition, the FSS matched and filtered the rectenna system much better than state-of-the-art rectenna systems implementing stub-matched transmission line filters (see Table 9.1).

For the rectification circuit used in the rectenna design presented, two approaches were considered. First, the standard single diode placed in parallel was tested. Afterwards, a dual-diode system was used. In the dual-diode rectification, a diode was placed in series across each transmission line prior to the termination across the load resistor. Once both approaches were measured and analyzed, it was conclusive the dual diode approach first demonstrated in (Ren and Chang, 2006) proved to yield a more efficient AC-to-DC conversion and therefore ultimately a higher RF-to-DC conversion efficiency when implemented within a rectenna system.

In the last stage of the rectenna system, various load resistances were tested until a load resistance yielding the highest output voltage and RF-to-DC conversion efficiency was found.

Chapter 2

Rectenna History

2.1 History: Development of Rectenna Systems

The idea of wireless power transmission was presented by Nicolas Tesla over 100 years ago. Although Tesla was not able to successfully commercialize wireless power transmission, he was able to successfully transmit and receive power from prototype transmitters made with 150 kHz oscillators to two light bulbs hundreds of meters away. It is believed his attempt of wireless power transmission did not work on a larger scale because the 150 kHz signal radiated isotropically instead of being directed towards the receivers, the wavelength of the wireless system being approximately 20 km, and the efficiency of the system ultimately not being sufficient for recovery. (Vera, 2009)

Later in the 1950s, B. C. Brown of the Raytheon Company began experimenting with high-powered microwave power transmission. An efficient prototype for receiving and rectifying microwave power was finally produced in 1958, however this was paired with a 15 kW microwave tube with a DC-to-RF conversion of efficiency of 81% on the transmitting end of the system. This lack of efficiency on the transmission end limited the commercial viability of this prototypical wireless power system. (MHS, 2008)

Improving upon the reception and rectification of wireless power transmission systems, Raytheon developed a half-wave dipole rectenna using a single diode rectification also known as a balanced bridge (Vera, 2009). The rectenna was designed for 2.45 GHz operation, at the center of the Industrial, Scientific and Medical (ISM) frequency band.

The highest recorded RF-to-DC conversion efficiency was achieved by Raytheon Company in 1977(MHS, 2008). The rectenna system recorded a 90.6% conversion efficiency using aluminum bars as the dipole antenna element and was then rectified across a gallium arsenide

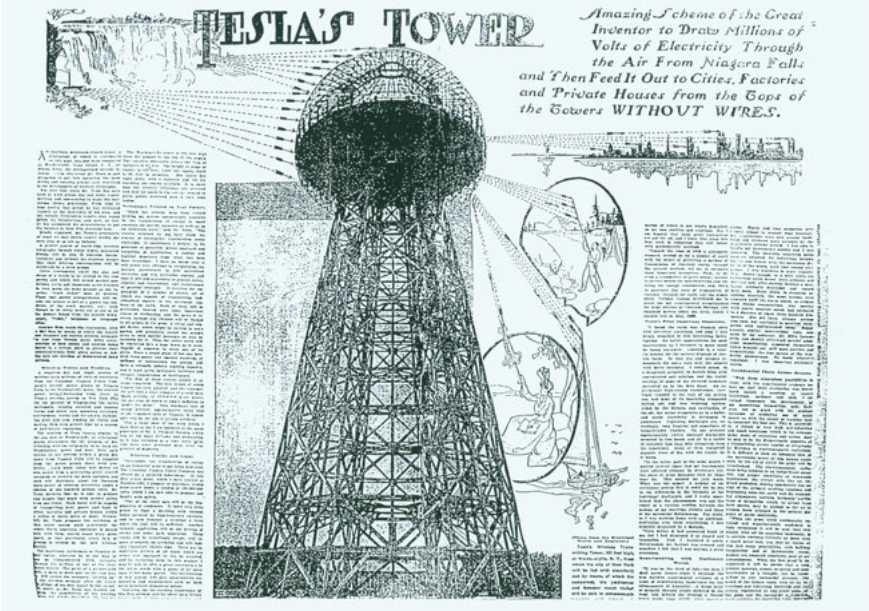

Figure 2.1: Newspaper boasting Tesla's tower being capable of powering residential and commercial settings(New York, 1904)

barrier diode. It should be noted that the rectenna was driven with an incident power level of 8 W/m^2.

Raytheon and NASA worked together on the development of several such rectenna systems in attempt to develop a Stationary High Altitude Relay Platform (SHARP). The SHARP system was proposed to capture solar energy using solar panels (Wu, Choudhury, and Matsumoto, 2013).

Once converted to an electrical signal, the SHARP system would then transmit the energy to a ground-based station via microwave power transmission. The microwave energy would then be received via a rectenna system and converted to usable DC power. Ideally, the SHARP system would relay energy from the sun to the Earths surface without any hindrances and would provide a seemingly limitless source of free energy. However, the high power nature of the microwaves beamed to the Earths surface proved to be hazardous and even deadly for aerial travelers, vehicles and animals.

In 1982, Brown introduced a low-power, thin film version of the rectenna printed on flat substrates. (Brown and Triner, 1982)

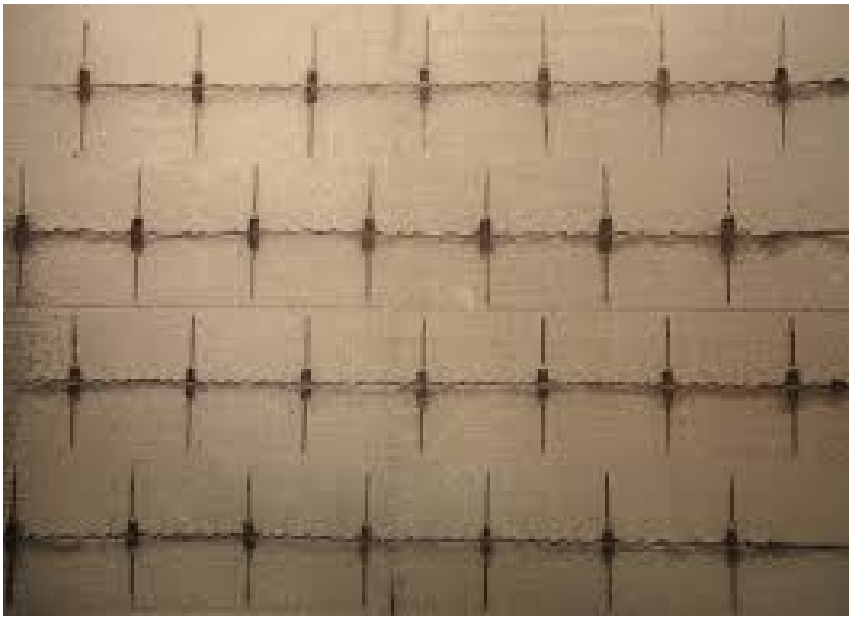

Figure 2.2: Aluminum Antenna Elements used for Raytheon's Record Rectenna (MHS, 2008)

2.2 Impactful Work

The pioneer and man responsible for laying the framework of microwave power transmission is undoubtedly W.C. Brown. The progress seen in modern wireless power transmission is directly attributed to the contributions Brown made during his tenure with the Raytheon company (MHS, 2008).

After graduating with a bachelors degree in electrical engineering from Iowa State University, Brown was hired to work for the Radio Corporation of America (RCA). It was while working at RCA that Brown gained experience in working with high-powered vacuum tubes. After his time as a trainee at RCA, Brown accepted a scholarship from the Massachusetts Institute of Technology (MIT) and soon after accepted a job in 1940 working for Raytheon Company. During his time at Raytheon, Brown was assigned the task of helping improve World War II radar systems. The radar systems at the time used magnetrons, power generators using primitive oscillators, for radar transmission. These magnetron-based radar systems were not considered suitable for military operation anymore. Helping this cause, Brown invented the Amplitron, a cross-field amplifier, adapting the magnetron oscillator to

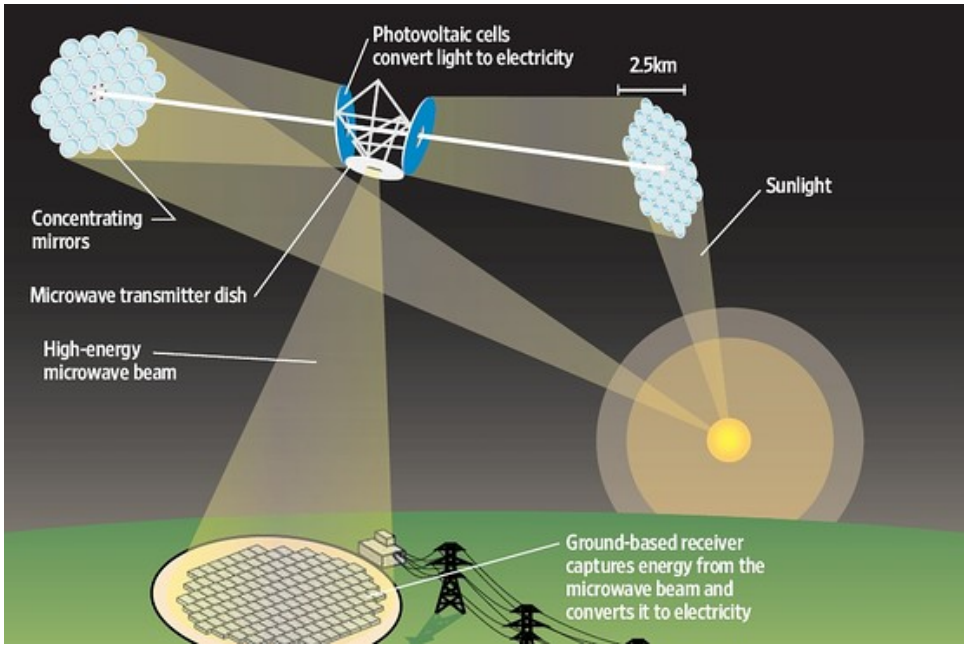

Figure 2.3: Stationary High Altitude Relay Platform (SHARP)(Yuwei et al., 2010)

serve as a broadband amplifier (MHS, 2008). This cross-field amplifier was the first of its kind and went on to be used in navy radar systems(Aegis), missile systems(Hawk and Patriot), commercial airline monitoring systems and even the higher-frequency communication systems used in the Apollo missions.(MHS, 2008)

After developing the Amplitron, Brown began working on microwave power tranmsmission systems. Beginning with his prototype rectenna developed in 1958 designed for receiving energy transmitted from a 15 kW 2.5 GHz microwave source, Brown began laying the stepping stones towards a more efficient method of receiving incident microwave energy (MHS, 2008)(Wu, Choudhury, and Matsumoto, 2013). As the capturing and conversion of inbound microwave energy is the essential to microwave power transmission, development of the device comprised of an antenna and rectification circuit or "rectenna" was a highly influential milestone in the advancement of wireless power transmission and is the key element in developing microwave power transmission and energy harvesting systems today.

Demonstrating his progress made since the rectenna prototype, Brown revealed a microwave energy powered helicopter on the CBS Walter Cronkite news in 1964. The helicopter

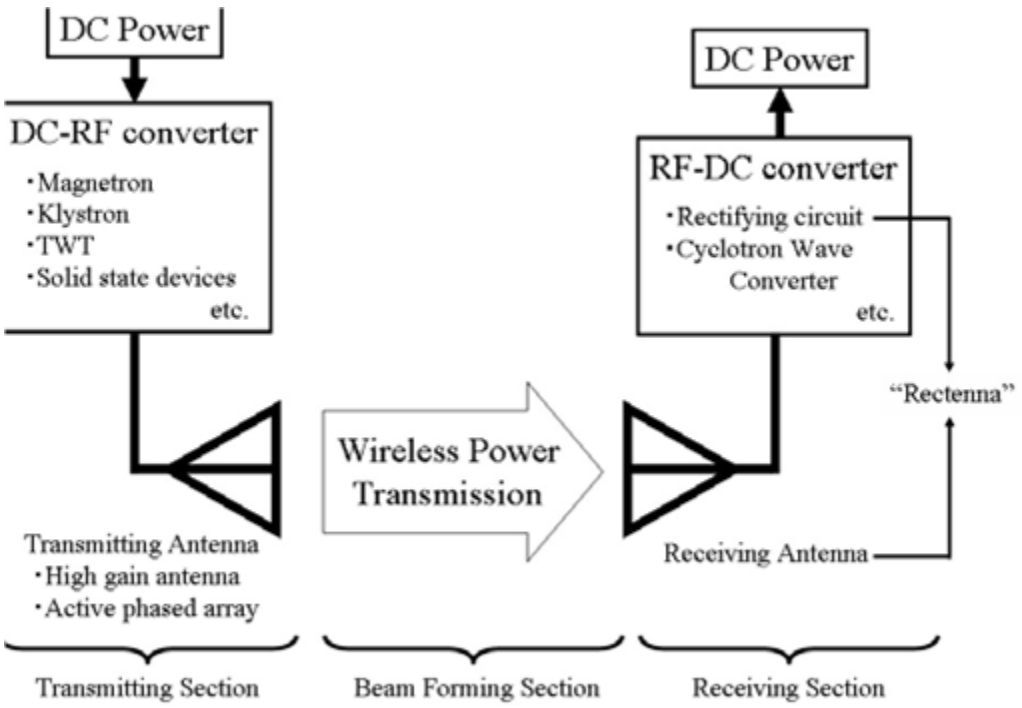

Figure 2.4: Primitive Tube-based Microwave Power Transmission System (Mitani et al., 2006)

was basic in that it consisted of only a propeller and 2.45 GHz rectenna elements, however he was able to power the helicopter for 10 continuous hours of flight using microwave energy converted to DC power. (MHS, 2008)(Donchev et al., 2014)

In 1969, Brown received his patent for the RF-to-DC converter used in microwave power transmission. Furthermore, in 1975, as a technical director of a joint program between Raytheon and the Jet Propulsion Laboratory (JPL), Brown was able to construct a microwave power transmission system using a high-powered vacuum tube source and ultimately received energy at an efficiency of 54% from a mile away.(MHS, 2008)

At the time, Brown used microwave tubes as transmission sources due to their availability at the time as well as their high power output. Today, most microwave power transmission systems use a high powered antenna or antenna array to transmit energy towards the rectenna where the microwave energy is to be captured and converted to usable DC power.

These advances antenna design have helped provide a much more directive transmission system in microwave power transmission systems, making the overall system much more

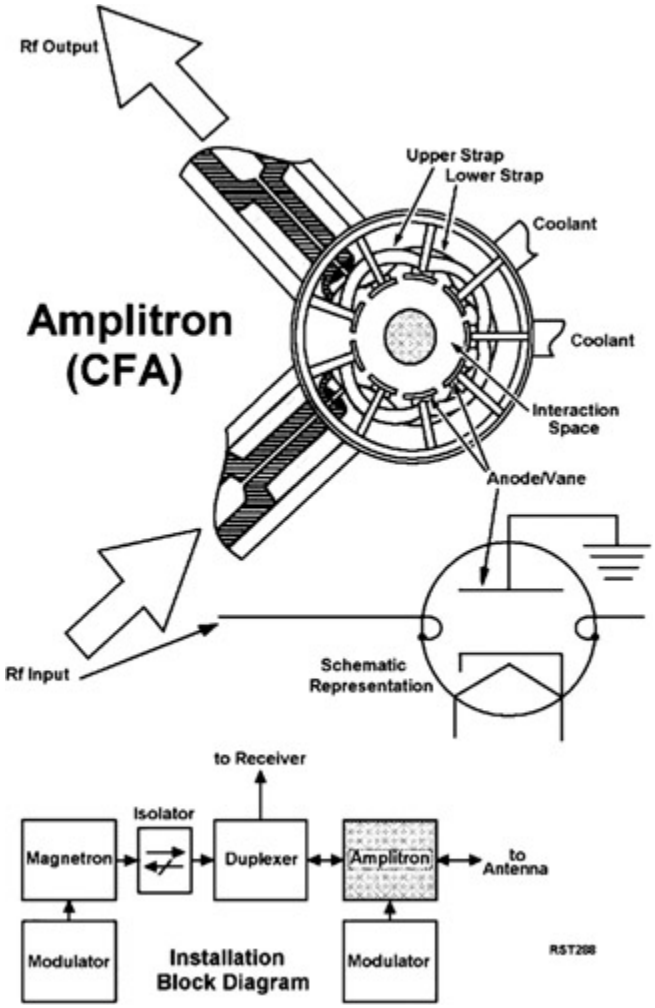

Figure 2.5: W.C. Amplitron (Bouwman, 2008)

efficient. In microwave power transmission systems, the more directive the source is, the less energy is scattered into free space or medium the energy is propagating through. In a highly directive system, it is ensured more microwave energy will arrive incident upon the effective aperture of the receiving end of the wireless power transmission system.

On the receiving end of these systems, a rectenna is the essential device which receives and converts the incident energy to supply level DC power. Comprised of an antenna, rectification circuit and often a filter/matching network of some sort, the antenna element serves the primary role in capturing incident microwave energy.

In microwave power transmission systems, an overall directive system is desired both in

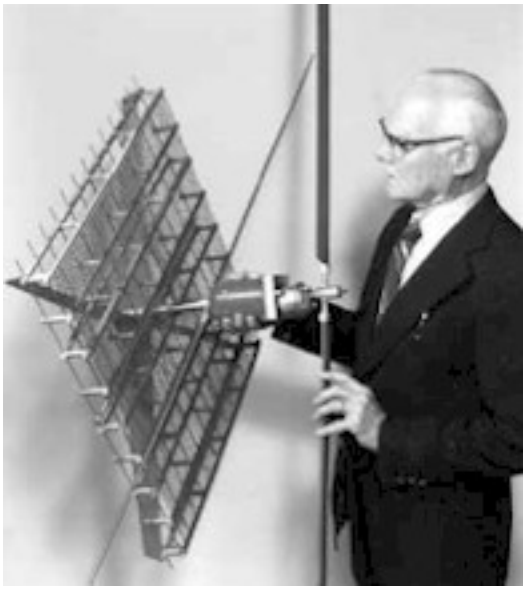

Figure 2.6: W.C. Brown's Microwave Powered Helicopter (Donchev et al., 2014)

terms of the antenna on the transmission side of the power transmission system as well as the energy reception taking place at the rectenna on the receiving end of the power transmission system. Having more directive antenna systems on both ends ensures less noise will be introduced within the path between the two antennas and less microwave energy to be attenuated from transmission to reception. This enhanced directivity plays a significant role in recovering a greater portion of the beamwidth radiated from the transmission source and is therefore a paramount factor when designing wireless power transmission systems.

Contrary to microwave power transmission systems, wireless energy harvesting systems also often referred to as energy scavenging systems, require a much different performance in terms of what is asked of the antenna used within the rectenna. Due to the nature of their application, microwave energy scavenging systems benefit from being capable of capturing microwave energy from potential sources in all directions. Because there is often no defined location or single source from which these systems will receive their microwave energy, rectennas developed for these receiving systems profit from the use of an omnidirectional antenna or antenna system. This omnidirectionality allows for the energy harvesting system to capture and convert energy from more of the unpredicted microwave energy sources and

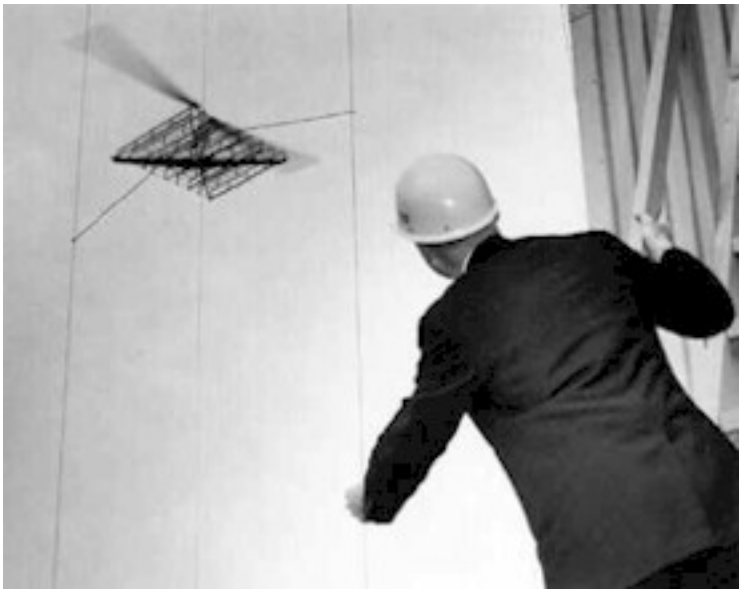

Figure 2.7: W.C. Brown's Microwave Powered Helicopter in Flight (Donchev et al., 2014)

thus provide a greater amount of converted power to the load or device which the rectenna is designed to deliver power to.

The primary component of a rectenna system is the antenna. In the past, most antenna designs observed were typically aperture antennas such as horns, cones or other three-dimensional structures. Subsequently, rectennas consisted of the same type of antennas. However the evolution of antenna design and RF engineering as a whole brought forth the era of planar antenna elements known as microstrip antennas.

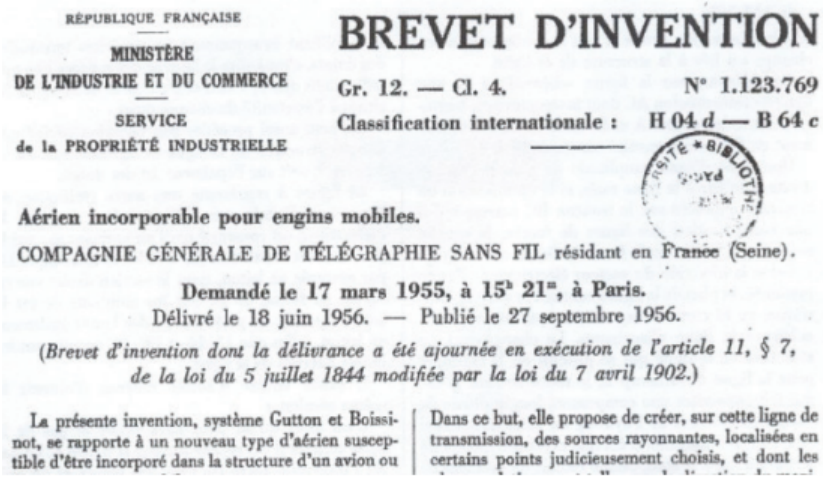

RÉPUBLIQUE FRANÇAISE

MINISTÈRE
DE L'INDUSTRIE ET DU COMMERCE

SERVICE
de la PROPRIÉTÉ INDUSTRIELLE

BREVET D'INVENTION

Gr. 12. — Cl. 4. N° 1.123.769

Classification internationale : H 04 *d* — B 64 *c*

Aérien incorporable pour engins mobiles.

COMPAGNIE GÉNÉRALE DE TÉLÉGRAPHIE SANS FIL résidant en France (Seine).

Demandé le 17 mars 1955, à 15h 21m, à Paris.

Délivré le 18 juin 1956. — Publié le 27 septembre 1956.

(Brevet d'invention dont la délivrance a été ajournée en exécution de l'article 11, § 7, de la loi du 5 juillet 1844 modifiée par la loi du 7 avril 1902.)

La présente invention, système Gutton et Boissinot, se rapporte à un nouveau type d'aérien susceptible d'être incorporé dans la structure d'un avion ou

Dans ce but, elle propose de créer, sur cette ligne de transmission, des sources rayonnantes, localisées en certains points judicieusement choisis, et dont les

Figure 2.8: First Microstrip Antenna Patent (Peixeiro, 2011)

The first case of a microstrip patch antenna was documented when in 1955, a French patent by Gutton and Bussinot claimed the invention. The intellectual property presented belonged to the Federal Telecommunications Company of France. The First unclassified publication of a Microstrip Antenna was presented in the IEEE Transactions on Antennas and Propagation in 1974 by Deschamps and Sichak who also worked for the Federal Telecommunications Company of France. (Peixeiro, 2011)

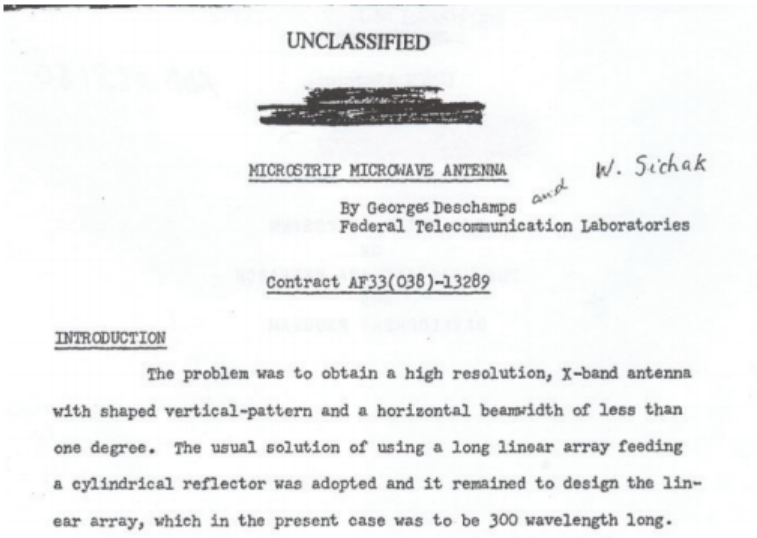

UNCLASSIFIED

[redacted]

MICROSTRIP MICROWAVE ANTENNA

By Georges Deschamps and W. Sichak
Federal Telecommunication Laboratories

Contract AF33(038)-13289

INTRODUCTION

The problem was to obtain a high resolution, X-band antenna with shaped vertical-pattern and a horizontal beamwidth of less than one degree. The usual solution of using a long linear array feeding a cylindrical reflector was adopted and it remained to design the linear array, which in the present case was to be 300 wavelength long.

Figure 2.9: First Microstrip Antenna Publication (Peixeiro, 2011)

Since Deschamp and Sichak's introduction of the microstrip antenna was published in 1974, the use of planar antenna alternatives began to steadily grow within academic and commercial research. A 1981 "special issue" on microstrip patch antennas in IEEE Transactions on Antennas and Propagation sparked a notable growth in the development of these antennas within the antenna community. A significant increase in the number of microstrip antenna publications has been observed since 1981 and is still booming as applications of microstrip antennas has greatly increased in recent years.(Peixeiro, 2011)

Microstrip or "patch" antennas provide conformal design, easy fabrication, and scalability in terms of developing planar antenna arrays. Building upon the notion of scalability, patch antennas are also printed on dielectric substrates varying in electrical permittivity.

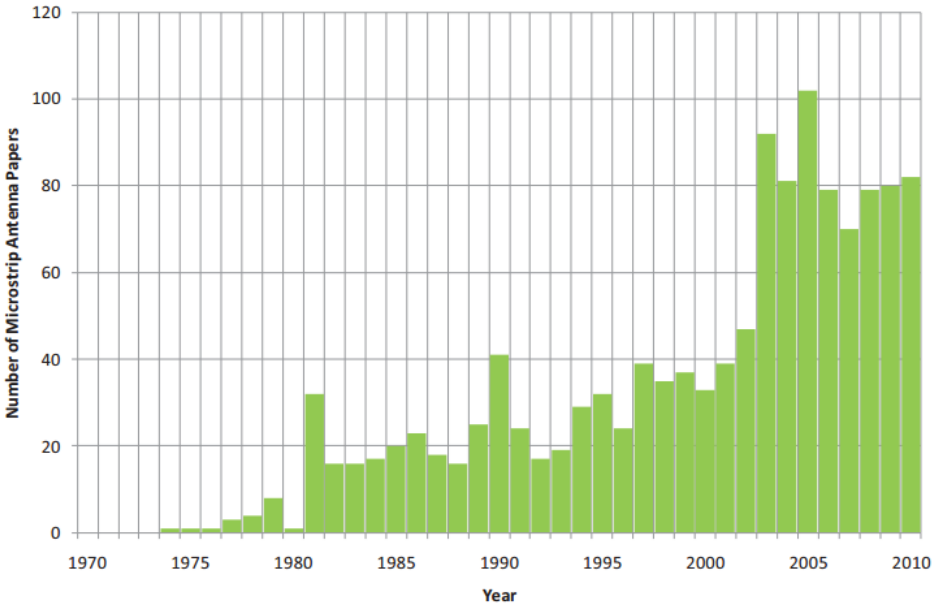

Figure 2.10: Growth of Microstrip Antenna Publications From 1974-2010 (Peixeiro, 2011)

Available in a variety of permittivities, the resonant wavelengths of the geometries printed on them may be shortened if fabricated on substrate mediums with higher electrical permittivities. They are also often fabricated on flexible substrates allowing for conformal designs to be applied in a variety of durable applications.

Due to the mentioned advances made in antenna design, the increased exposure of the research area and the development of the patch antenna, in 1982 B.C. Brown, already a pioneer within microwave power transmission, developed one of the first thin-film printed rectenna designs. Made using a microstrip antenna, the rectenna printed on a kapton substrate measured with an RF-to-DC efficiency of 85% (Brown and Triner, 1982). The development and publication of this microstrip rectenna opened the door for an array of future thin-film rectenna applications. Several of these uses are provided in the next chapter, Rectenna Applications.

2.3 State of the Art

Many current state-of-the-art microwave energy scavenging systems utilize patch antennas typically operating in the microwave band from 1 - 8 GHz (Donchev et al., 2014). Patch antennas are conformal to planar surfaces and have a relatively small form factor for their respective aperture. They are also easily fabricated and the necessary impedance matching networks and filters are placed in the adjacent space to create compact designs (Ren and Chang, 2006), (Hong et al., 2010), (Lee and Chang, 2015).

Ren et al. (2006) designed a 5.8 GHz dipole square patch rectenna using dual-series diode rectification. The 1.35 λ long antenna used a combination of stub matching, transmission line filtering and a novel dual-diode half-wave rectifier to provide an RF-to-DC conversion efficiency of 76% and DC output of 6.22 V (Ren and Chang, 2006).

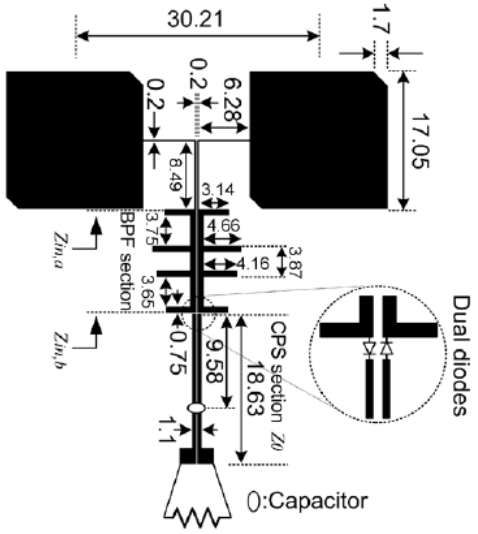

Figure 2.11: 5.8 GHz Dual-diode Patch Rectenna - (Ren and Chang, 2006)

This was one of the first times such a rectification method was applied to a rectenna configuration in a published work. Typically, a single shunt diode was used for the rectification circuitry, however in this paper, Ren et al. applied the dual-diode rectification concept to their patch rectenna design. Although a full-wave rectification would be ideal in theoretical application, the development of a full-wave rectifier on an RF substrate would require

a significant amount of surface area. This was acknowledged in the paper and instead the dual-diode system was presented.

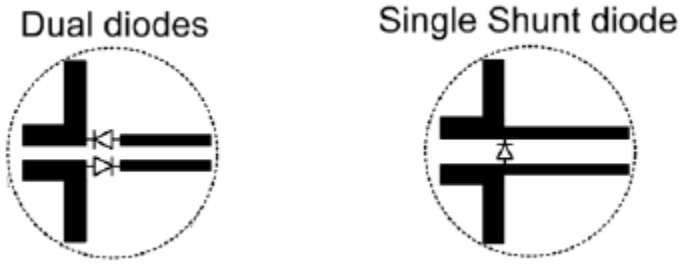

Figure 2.12: Single-Shunt vs Dual Series Diode (Ren and Chang, 2006)

The dual-diode rectifier circuitry used in the rectenna design present by Ren et al. consists of two RF Schottky barrier diodes placed in series with the dipole antenna's transmission lines. When compared to the often seen single-shunt diode rectification, the measured voltage output of the rectenna is proven to be almost double that of the single-shunt diode rectification. Later in this work, the RF-to-DC efficiency of the two rectification approaches are compared as well and it is clear the dual-series-diode rectification yields a more efficient conversion efficiency.

The use of this dual-diode rectification has proven to be extremely effective since publication. Application of this dual-diode rectification keeps the cost and simplicity of the rectification circuitry at a minimum while eliminating the necessity for voltage doublers and full-wave rectifiers. Kai Chang, one of the authors of the paper, adopts the dual-series-diode rectification in several other publications and continues to apply the circuitry to several other rectenna designs as well. (Hong et al., 2010)(Lee and Chang, 2015)

Hong et al. (2010) constructed a 2.45 GHz monopole rectenna for energy harvesting. Their design used stub matching, transmission line filter and single-diode rectifier. The 1.2 λ long monopole achieved a conversion efficiency of 66% and maximum DC output of 2.6 V at 2.45 GHz. (Hong et al., 2010)

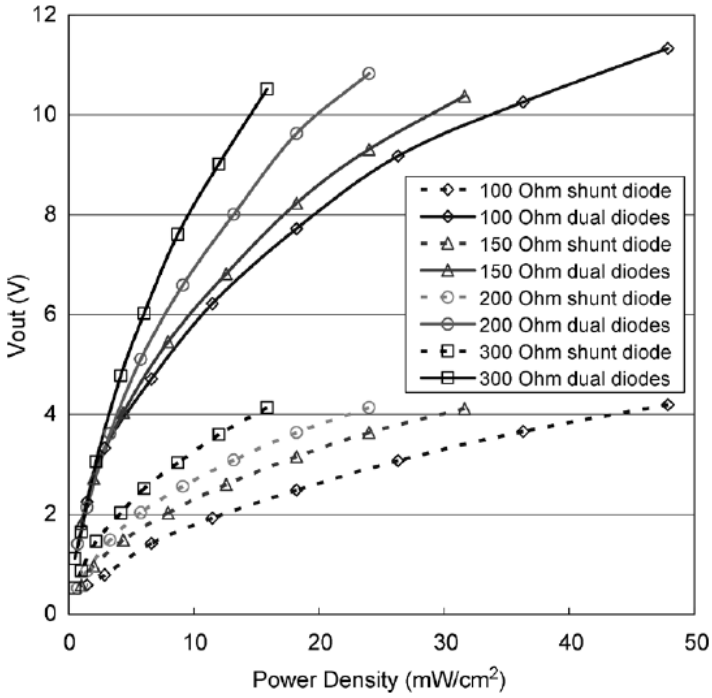

Figure 2.13: Output voltages for both rectifications (Ren and Chang, 2006)

In 2015, Lee and Chang introduced an efficient broadband printed dipole rectenna centered at 6.3 GHz. Using transmission line filtering and vias, the multi-layered design was 4.89 λ in length and provided a maximum RF-to-DC conversion efficiency of 81% using a single-diode half-wave rectification and maximum DC output of 1.98 V at 5.6 GHz [14].

The research presented here focuses on energy scavenging at the ISM band (2.45 GHz) using a patch antenna rectenna design. The rectenna incorporates a vialess multi-layered structure and replaces typical stub matching networks and transmission line filters with a Frequency Selective Surface (FSS).

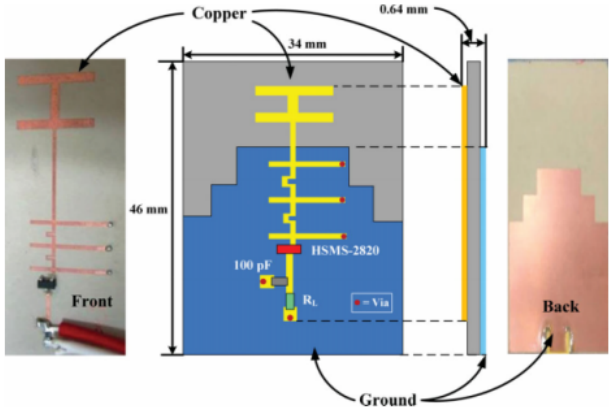

Figure 2.14: 2.45 GHz Monopole Rectenna (Hong et al., 2010)

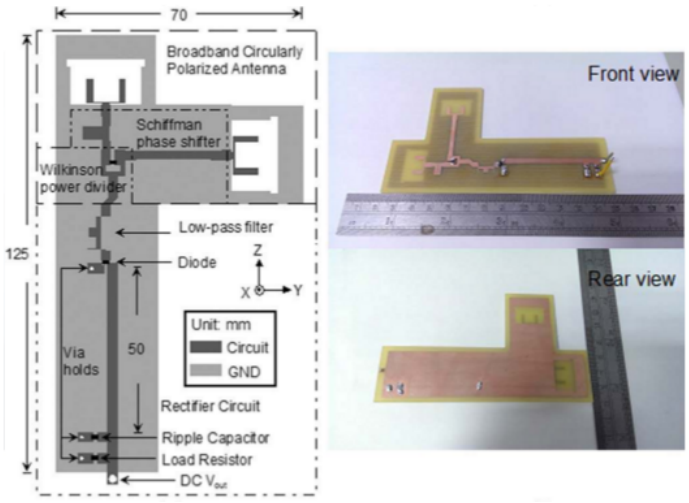

Figure 2.15: Broadband Printed Dipole Rectenna - (Lee and Chang, 2015)

Chapter 3

Rectenna Applications

In recent years, significant progress has been made in microwave power transmission. Short range powering applications typically uses inductive transformer action and applications of this are often seen in the charging of household appliances such as phones and toothbrushes. Far-field microwave powering typically uses directional high-powered transmission and a variety of its low, medium, and higher powered applications are presented in this chapter. The emergence of Radio Frequency Identification (RFID) and along with its dependency on rectenna systems has developed significant research interest in recent years. Subsequently, rectenna-based energy harvesting and power transmission systems have benefited as a result.

Barcode	**RFID**
Require line of sight to be read	Can be read without line of sight
Can only be read individually	Multiple tags can be read simultaneously
Cannot be read if damaged or dirty	Can cope with harsh or dirty environments
Can only identify the type of item	Can identify a specific item
Cannot be updated	New information can be over-written
Require manual tracking and therefore are susceptible to human error	Can be automatically tracked removing human error

Figure 3.1: Comparison of barcode scanning vs RFID (Brown, 2010)

Due to the continuously growing inventories associated with present retailers, the management, tracking and control of retail products has become quite a challenge. Warehouses and stores often house thousands of various retail items and identifying the locations and availabilities of each item in or out of stock can become problematic. Previously, these items were managed using a barcode scanning method which involved manually reading the code

label printed on each retail item individually from a close distance. Replacing this and other outdated systems, RFID has proven to be a superior alternative. (Sothcott, 2011)

An adaptation of a microwave power transmission system, an RFID system uses a transmission source as well as a rectenna on they receiving end. The energy incident on the rectenna element by a RFID reader, consisting of a transmitting antenna as well as a receive antenna used to relay identification numbers or information from the targeted receiver. The receivers are referred to as RFID tags, and when designed as passive devices, they are true rectennas; consisting of an antenna, rectification and load. The RFID tag captures the incident energy and once converted, is used to relay information such as an identification number from either a DC powered integrate chip or similar memory-based load.

Compared to the optical based barcode system previously used, RFID systems allow for a multitude of items to be located and identified almost simultaneously. However the RFID applications of wireless power transmission is hardly limited to the commercial environment. Wireless sensor networks have seen have demonstrated a significant presence ever since the popularity of RFID has grown.(Sothcott, 2011)

Figure 3.2: Intel RFID tag placed on honey bee (Electronics360, 2015)

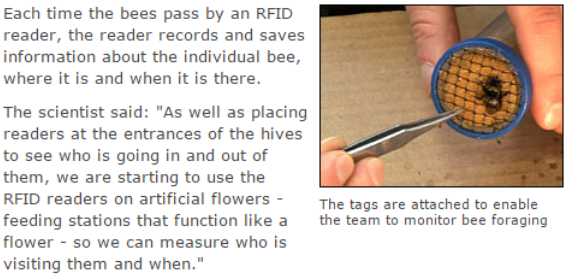

Figure 3.3: RFID used in tracking bee activity and monitoring beehive populations (Morelle, 2008)

Wireless sensor networks benefiting from the use of rectennas and RFID technology have quietly revolutionized our way of life through the various impacts they have had on our society. Tracking of endangered animals using RFID tags allows for population control and helps prevent extinction of currently endangered species. Within agriculture, wireless sensors are used to monitor the health and progress of livestock from a central database, simplifying the job of farmers. Packaged foods in supermarkets now contain printed RFID tags with sensors which detect if meat or poultry has been contaminated with salmonella. Within warfare, RFID is used to identify friendly targets and prevent friendly fire. It also may be used for tracking and determining the locations of personnel. (Sothcott, 2011)

Figure 3.4: Meat Product with RFID Sensing Food Safety Label ("4210 EP Food Label")

The development of rectenna systems, including RFID, have increased the public's familiarity with microwave power transmission systems and led to the application of rectenna elements in numerous more commercial and military applications. Applications such as providing energy for helicopters and airplanes, relaying energy from space to earth using a solar-powered to microwave power transmission system, powering space instruments and satellites, powering motors and short-to-medium range wireless power transfer systems both on land and space have been proposed. (Sothcott, 2011)

Figure 3.5: Airplane powered via a Stationary High Altitude Relay Platform (SHARP) (Wilson, 2015)

Even within the medical field, applications of wireless body sensors are beginning to make a significant impact. Especially in sensitive in-vitro applications where inserting an unreachable power supply of some sort is not desirable, remotely powered wireless sensors are beginning to develop in life-saving applications. (Sothcott, 2011)

Diabetics who previously were forced to puncture themselves and bleed onto strips of paper to monitor glucose levels now have wireless sensor-based alternatives (Sothcott, 2011). Contact lenses with built in glucose sensors providing instantaneous glucose reading allow for sufferers of diabetes a pain free alternative to having to prick and bleed themselves (Sothcott, 2011).

People with subtle and severe food allergies may now have a way to prevent possible consumption of lethal doses of harmful products thanks to wireless sensors being implanted within tooth enamel (Sothcott, 2011). Sensing a wide range of materials such as gluten, lactose, e.coli or sodium, these sensors can prevent harmful consumption or even be used for keeping track of what a person eats. (Sothcott, 2011)

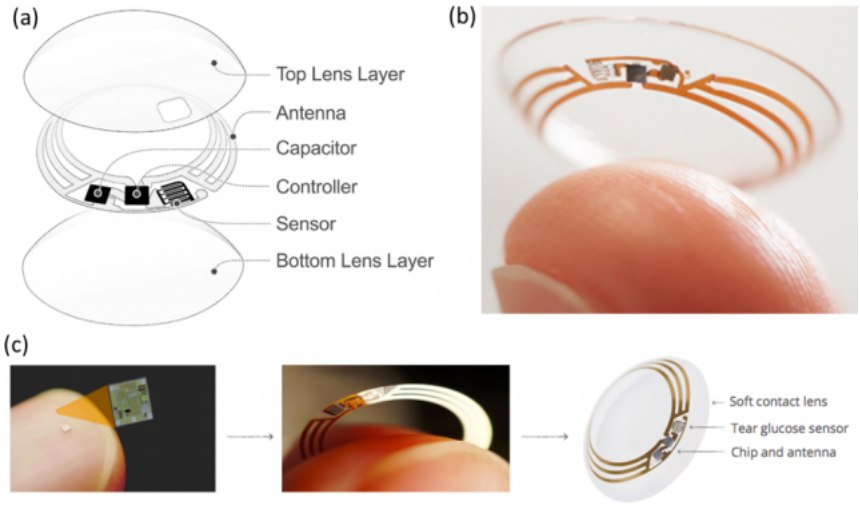

Figure 3.6: Wireless Glucose Sensing Contact Lens (Farandos et al., 2015)

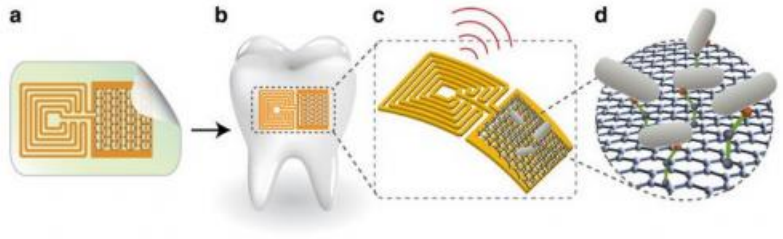

Figure 3.7: Wireless Sensing in Teeth (Mannoor et al., 2012)

In addition to being highly directive, rectenna systems used for microwave power transmission are circularly or elliptically polarized, allowing for a greater spatial power distribution and greater potential for incident power upon the receive rectenna. This ultimately yields a higher aggregate transmission/reception efficiency for the microwave power transmission system.

Contrary to polarization-sensitive directional microwave power transmission systems, energy scavenging or harvesting systems use omnidirectional antennas for capturing ambient and semi-ambient microwave energy. Because SNR is not important in energy scavenging systems and ideally all ambient microwave energy is to be received and converted to DC power, a somewhat universal polarization is beneficial in the rectenna design. Because most

ambient and reflected energy is typically linearly polarized, a symmetrical linearly polarized design with inevitably decent cross-polarization is presented in this work (Vera, 2009) (Donchev et al., 2014).

Chapter 4

Frequency Selective Surfaces

Frequency Selective Surfaces (FSS) are often patterned, repetitive surfaces designed to absorb or reflect incident electromagnetic waves. The periodicity of these structures determines what frequency these surfaces operate at. Because of their frequency dependent operation combined with reflection and transmission properties, they may be referred to or characterized as filters. (Hooberman, 2005)

FSS filters may be developed as primarily inductive structures or primarily capacitive filters. Geometrical inverses of one another, they are compliments and behave as low pass filters as well as high pass filters due to their reciprocity.

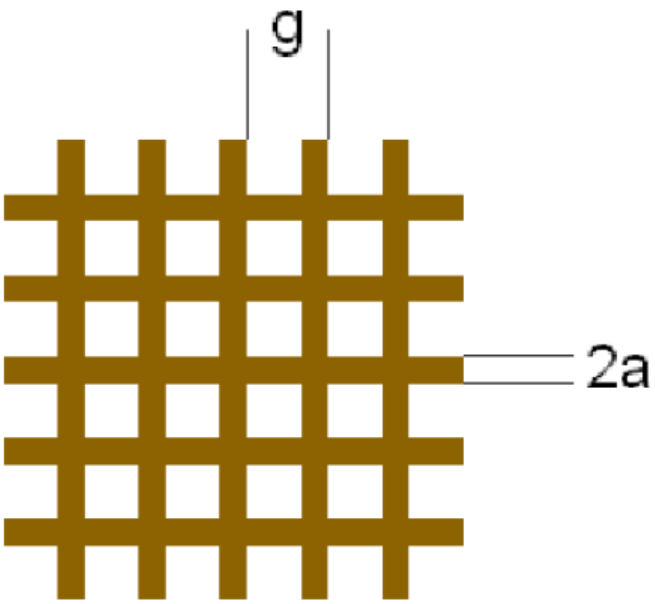

Figure 4.1: Inductive Mesh Filter (Hooberman, 2005)

A capacitive mesh FSS is comprised of an array of adjacent conductive square elements. The inductive mesh FSS is the inverse of this, a web of intersecting conductive metal lines

with square spacings between the lines. An advantage of using these FSS structures is that the polarization of propagating waves through these surfaces are independent from the source polarizations they are often interacting with.

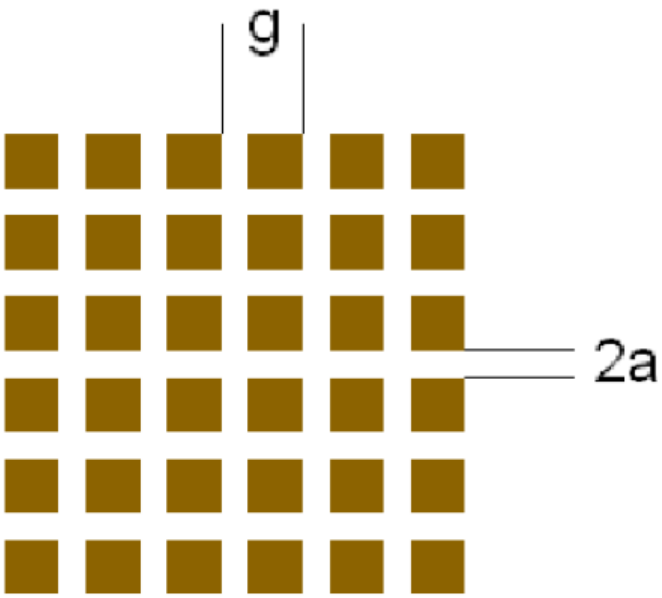

Figure 4.2: Capacitive Mesh Filter (Hooberman, 2005)

Due to the symmetry of the FSS design, if a linearly polarized wave was incident upon the surface, the FSS performance would behave the same if rotated by any 90 degree increment. This symmetry allows for fields to experience equal interaction when incident upon the FSS whether from a horizontal or vertical polarization.

In the inductive mesh FSS, because there are conductive paths across the entire surface, current is allowed to flow freely along the filter, allowing for lower frequency excitements to induce greater electron displacement and stronger reflection. (Hooberman, 2005)

Contrary to the inductive mesh filter, the capacitive mesh filter behaves in the opposite manner. Because each of the square patch elements of the FSS array are isolated, there is no observable route for current to flow amongst square patches.

Because of their filtering properties, there are several ways to model and analyze these surfaces. FSS sheets are often modeled in terms of their resistance, inductance and capacitance in the form of RLC circuits.

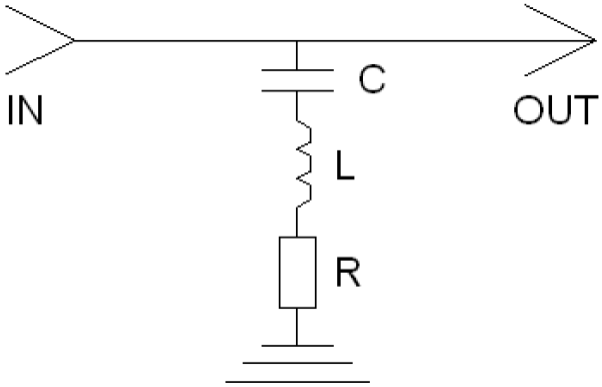

Figure 4.3: Inductive Mesh Circuit (Hooberman, 2005)

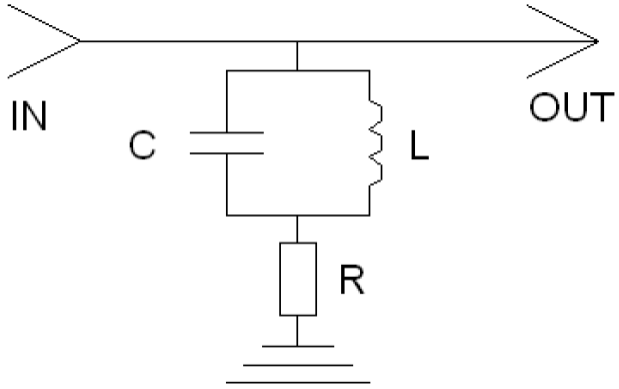

Figure 4.4: Capacitive Mesh Circuit (Hooberman, 2005)

Because these inductive and capacitive FSS filters may be analyzed as RLC circuits, the empirical formulations for the filters are provided in (Hooberman, 2005)

Of the two demonstrated FSS filters, the capacitive mesh filter consisting of square patches was selected for the multi-layered antenna and rectenna design presented in this work. Based on reviewed work, the capacitive FSS and its metal square patches not only provide greater reflection at "higher frequencies" according to (Cure, Weller, and Miranda, 2011), but also provide minimized back-lobing and diffraction when used as a ground plane filter underneath an antenna or radiator.

Another possible geometry often used in FSS filters is the cross. the application of this FSS is identical to that of the square patch FSS structures. The cross patterned FSS, is exactly like the square patch FSS in that is consists of an array of repeating elements on its

surface, however the repeated element is a cross instead of a square. Like the square mesh filters, the cross mesh filters also have a version where they behave more as inductive mesh filters and a complementary capacitive mesh filter.

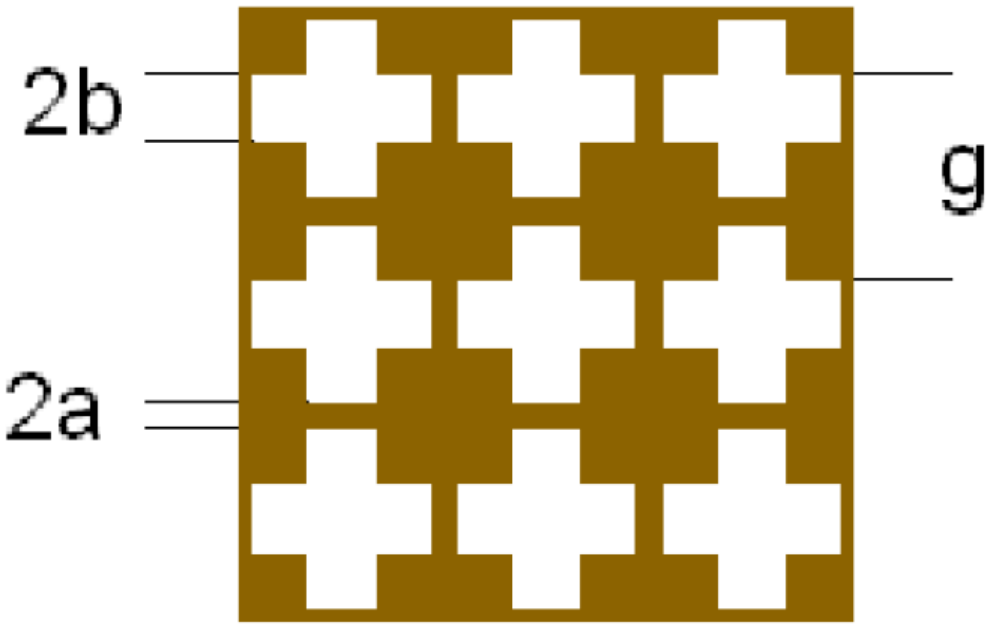

Figure 4.5: Inductive Cross Mesh (Hooberman, 2005)

In the capacitive cross mesh filter, the crosses are made of conductive material and the inverse is seen in the case of the inductive cross mesh filter. Similar to what is observed for the square patch FSS, the polarizations of these cross mesh filters are independent of the polarization of the source field incident upon the FSS. Because the geometry of the cross as well as its array is symmetrical when a 90 degree rotation is applied to the FSS, the filter has the capability of filtering both horizontally and vertically polarized incident waveforms.

An empirical approximation of the resonant wavelength of the cross mesh filter is provided in (Hooberman, 2005).

Assuming the structures are ideal and sized to their resonant wavelengths, electromagnetic waves incident upon the surface of the capacitive cross mesh filter see zero transmittance and full reflection at the designed frequency of the cross mesh FSS. Contrary to this, if the

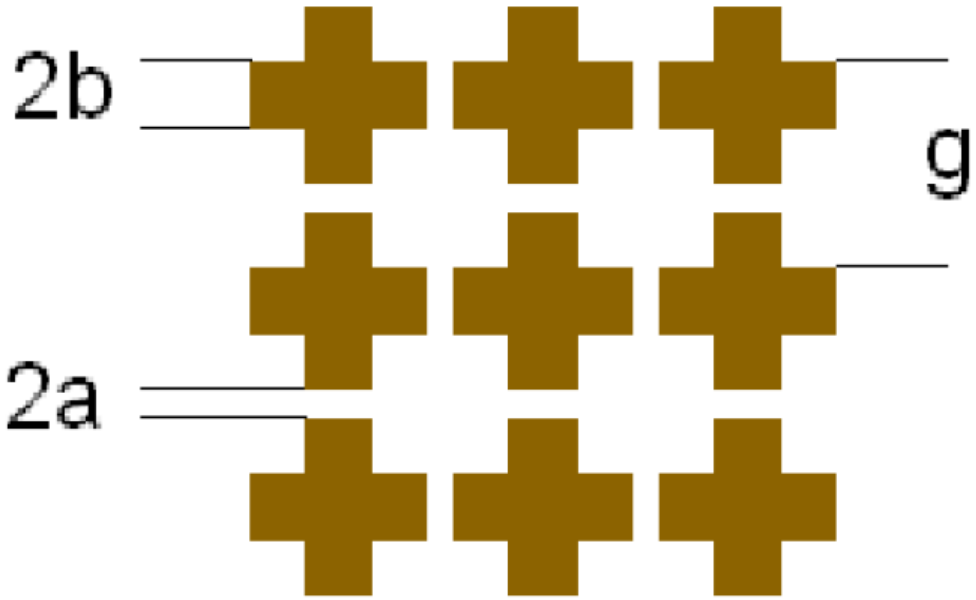

Figure 4.6: Capacitive Cross Mesh (Hooberman, 2005)

inductive cross mesh filter is ideal and designed to this resonant wavelength, waves incident upon its surface will see zero reflection and full transmittance.

The circuit models for the cross mesh filters were unavailable, however the admittances for the inductive and capacitive cross mesh filters are provided in (Hooberman, 2005).

A FSS comparison between the cross mesh filter and square patch mesh filter is provided in (Cure, Weller, and Miranda, 2011). In this work, the unit cell (each patch/element of the FSS) as well as the aggregate FSS element array is analyzed as a ground plance placed underneath an antenna element.

Using the full wave solver provided in the Ansoft "High Frequency Structural Simulator v15" (HFSS), the reflection and transmittance of the both the cross and square patch surfaces of the filter were analyzed.

It should be noted however than when the square patch is taken into consideration, the grid capacitance the inductance. This is demonstrated in the drawing denoting the equivalent model between two square structures as simply a capacitance.

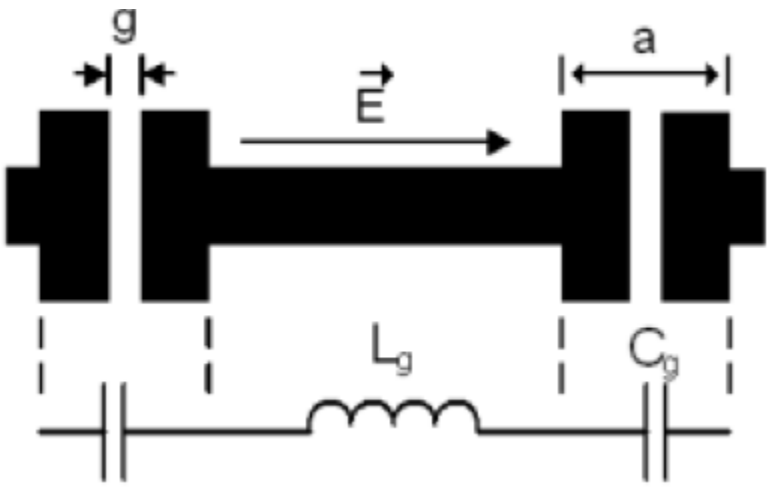

Figure 4.7: Layout and Equivalent Circuit Model of Theoretical Self-Resonant Grid (Cure, Weller, and Miranda, 2011)

If the capacitive mesh filter consisting of square patch elements is to be used for the FSS structure, the lack of inductive elements means the capacitance dominates the resonance of the structure. Due to this lack of balance, if a lower resonant frequency is desired for the FSS design frequency, larger square patch sizes must be used to increase the overall capacitance of the mesh filter to compensate for its lack of inductance.

Comparing the phase of reflection between the Jerusalem cross and square patch unit cells (individual elements) against an incident plane wave from above, Cure, Weller and Miranda (Cure, Weller, and Miranda, 2011) state that the bandwidths of each geometry begin and end approximately from when the phases of reflection reach the $-90°$ and $+90°$ values. The greatest impedance causing full reflection of incident waves is observed when the phases of reflection reach $0°$ and $180°$. Taking into account these observations, it is concluded the bandwidth of the square patch FSS is greater than that of the cross structure.

Further comparing the cross and square patch unit cells, the magnitudes of reflection of each have been simulated. In an ideal scenario, an incident plane wave would return a full reflection of $1\angle 0°$ and complete transmission of an incident wave would yield a $0\angle 0°$ in terms of magnitude of reflection. Comparing the magnitudes of reflection between the two

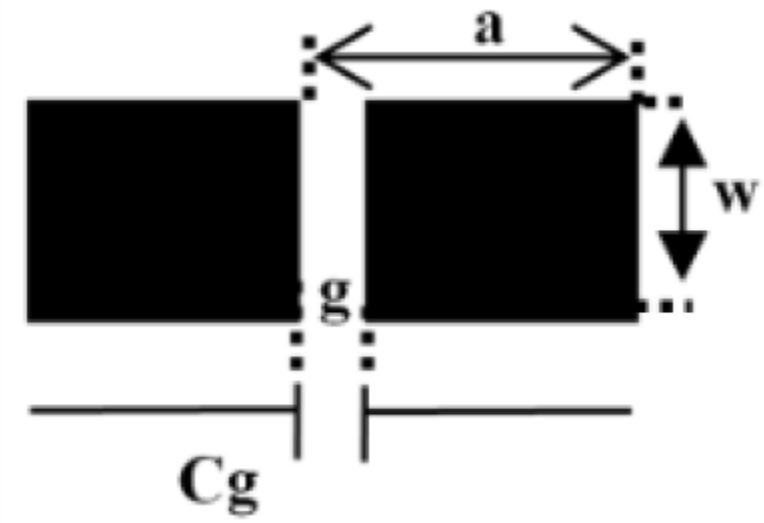

Figure 4.8: Layout and Equivalent Circuit Model of Theoretical Square Patch FSS (Cure, Weller, and Miranda, 2011)

geometries, it is concluded the square patch provides a much greater reflection relative to the cross structure.

The larger magnitude of reflection associated with the sqaure patch FSS as opposed to the cross geometry is theorized to be simply because a larger amount of surface area is covered with conductive metal in the case of the square patch capacitive mesh filter.

Based on the unit cell comparison, the higher reflection provided by the square patch element is believed to provide minimized leaked radiation through the bottom of the antenna placed above the FSS while also serving as a filtering device. (Cure, Weller, and Miranda, 2011) It is because of this greater reflection and its advantages that the capacitive square patch mesh filter FSS is chosen to be placed underneath the radiating antenna both in the reviewed publication as well as the antenna/rectenna presented in this work.

The rectenna presented in this work is a multi-layered design consisting of an antenna on the top layer with a FSS and ground plane below. Using the finite element and numerical method solver built into the HFSS electromagnetic structure simulator, the equations provided in this section are accounted for in the HFSS solver's computations. The capacitive mesh filter has been adopted as the FSS of choice for the rectenna design and is simulated

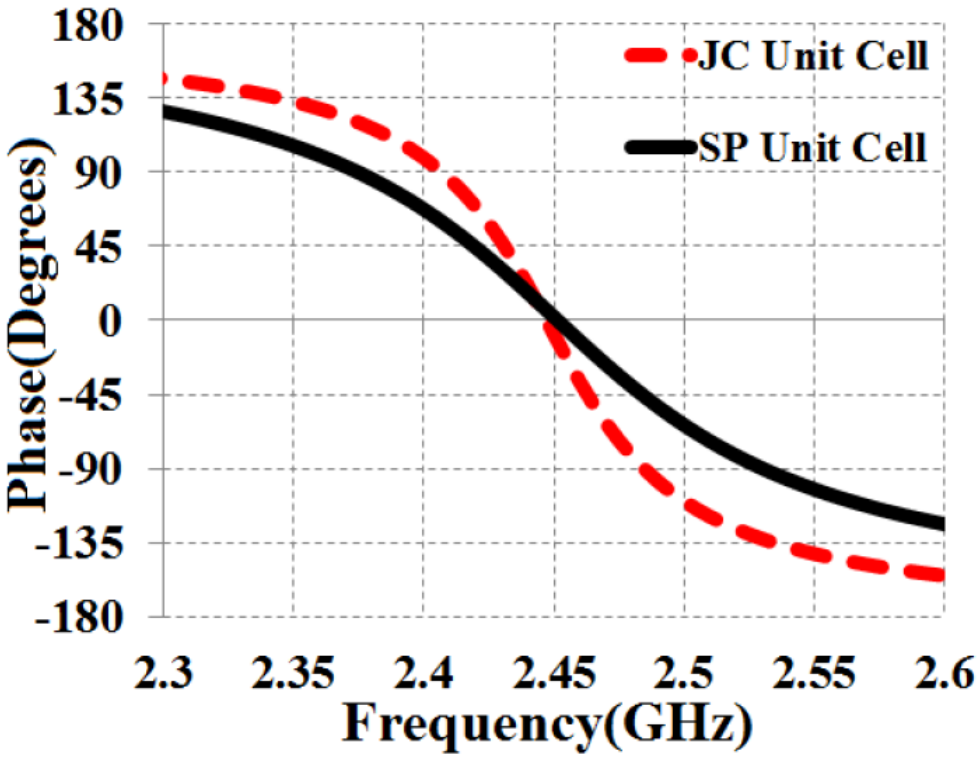

Figure 4.9: Phase of Reflection Coefficients for Cross and Square Patch Unit Cells in a FSS (Cure, Weller, and Miranda, 2011)

simultaneously along with the antenna on the top layer of the multi-layered rectenna design. Various sized spacings between elements as well as different sized square patches within the capacitive square patch mesh filter are tested using parametric analysis 5.6. This geometrical variation in itself tests various resonances for the grid-capacitance dominated resonant structure.

By simulating a sweep of values for the square patch sizes as well as the spacing between them, different values for the capacitance in the empirical models are being evaluated. Empirically, this may be versed as altering the dimensions, a and g, in equations 4.1 and 4.2. This ultimately yields different values for the grid capacitance in the FSS, C_g, altering the resonant frequencies and FSS bandwidths observed in equations 4.8 and 4.9. The results of this FSS Antenna simulation are presented in the next chapter and the measurements are provided in the Results chapter.

The application of the capacitive mesh filter within the rectenna design allowed for a

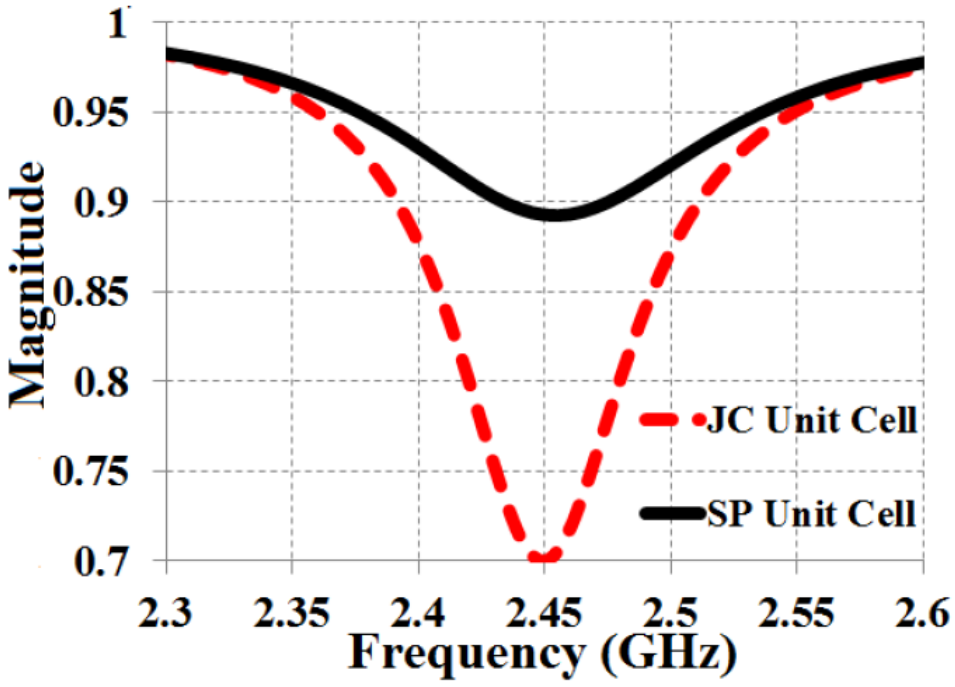

Figure 4.10: Magnitude of Reflection Coefficients for Cross and Square Patch Unit Cells in a FSS (Cure, Weller, and Miranda, 2011)

reduction in aggregate rectenna surface area. Where rectenna systems typically implement a filtering system via the use of stub matching and tee resonators, the FSS served as a filtering system in itself while occupying the same area as the ground plane of the antenna. In addition to filtering the multi-layered antenna presented, the FSS also provides a larger effective aperture to the antenna and ultimately the rectenna. This increased aperture with minimized diffraction through the ground plane was hypothesized to provide a beneficial broad radiation pattern towards capturing microwave energy within an energy harvesting application. The filtering and radiation performance of this design is confirmed and presented in the Results Chapter of this work.

Cell Type	*SP*	*JC*
Substrate thikness t (mm)	1.27	1.27
Unit Cell Length (mm)	15.1	11.76
Unit Cell Length reduction (%)	------	22
Unit Cell Area (mm^2)	228	131.3
Unit Cell Area reduction (%)	------	42.4
Unit cell BW (%) (±90°)	2.45	1.43
Min $\lvert\Gamma\rvert$	0.9	0.7

Figure 4.11: Comparison of Unit Cell Values for Cross and Square Patch Elements in a FSS (Cure, Weller, and Miranda, 2011)

Chapter 5

Rectenna

5.1 Frequency Selective Antenna

The rectenna presented uses a multi-layered dipole square patch antenna over a frequency selective surface and ground plane. The antenna has been designed to operate at a frequency of 2.45 GHz, the center frequency of the ISM band. This frequency was chosen due to the abundance of ambient energy radiated from electronic devices operating within this popular ISM band in commercial and residential environments. (Donchev et al., 2014)

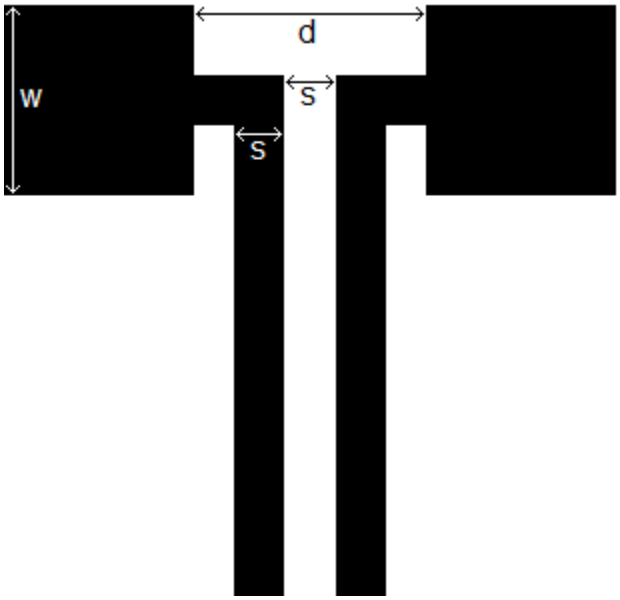

Figure 5.1: Dimensions of the dipole antenna

Using a multi-layered approach towards the rectenna design allows for a frequency-selective surface to be used in the rectenna system. This eliminates the increase in width and length of the overall rectenna structure as a stub matching system is no longer needed.

Table 5.1: Dimensions of the dipole antenna and frequency selective surface

w	**d**	**s**	**p**	**g**	**t**
16 mm	20.8 mm	1.6 mm	17.9 mm	.5 mm	92 mm

The FSS provides matching and tunes the antenna while occupying the same amount of surface area as a conventional ground plane.

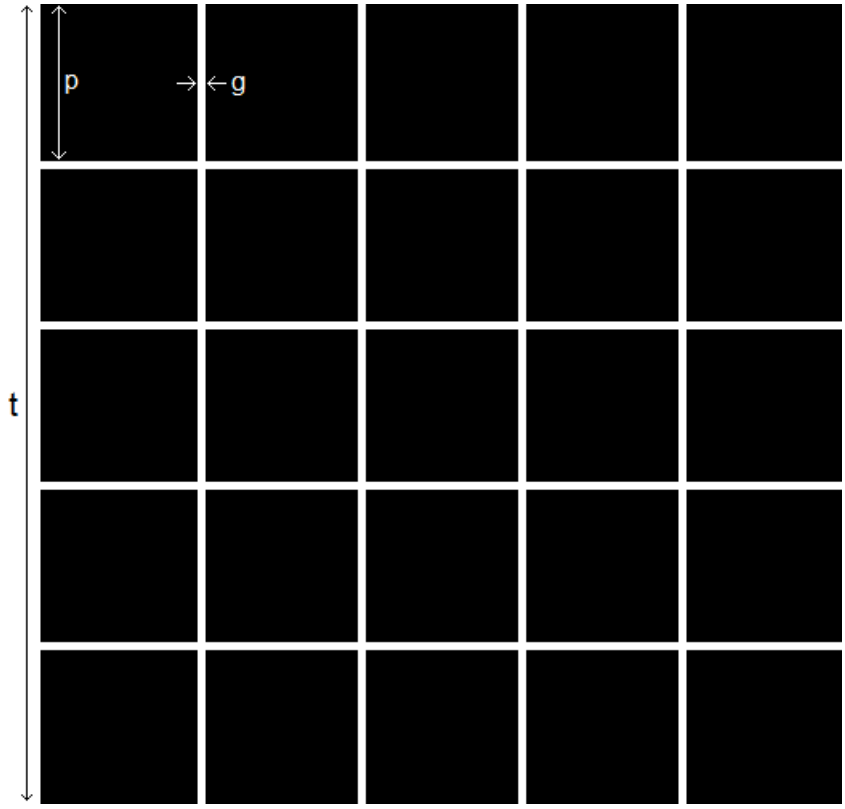

Figure 5.2: Dimensions of the frequency selective surface

This multi-layered approach saves a significant amount of area while improving matching when compared to transmission line filters found in similar patch rectenna designs.(Ren and Chang, 2006)

The top layer of multi-layer rectenna is copper and contains the patterned antenna, transmission lines, and rectification circuit (designated as the Antenna layer in Figure 5.4). The second layer is a Rogers 5880 dielectric substrate. The third layer is RF foam with an electrical permittivity approximately equal to that of air. This layer serves as a spacer between the Antenna element and FSS; where the distance between the two helps the FSS

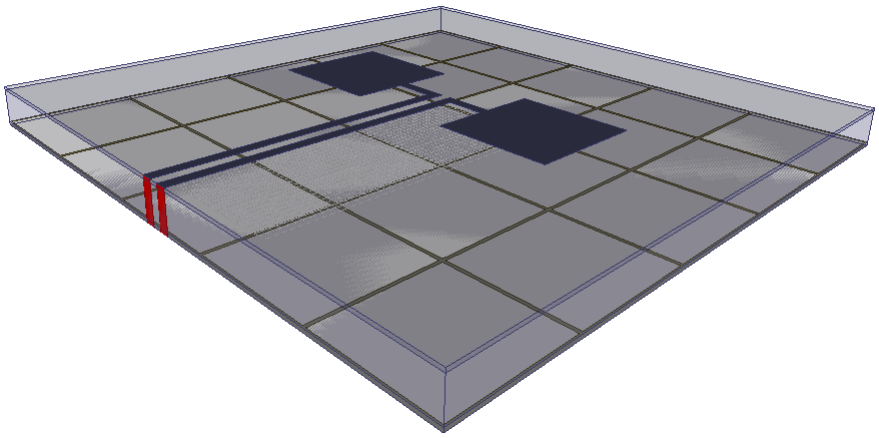

Figure 5.3: 3D view of FSS antenna model

tune the antenna above through constructive near-field coupling. The fourth layer is copper and contains the FSS; a periodic array of square patches. The fifth layer is Rogers 5880 dielectric substrate found in the second layer. The fifth layer is a copper ground plane; in place to further minimize back-lobing and produce a more efficient radiation pattern.

The dimensions of the designed frequency selective antenna are provided in 5.1, where w is the width of the antenna patches, d is the separation between the two patches of the dipole antenna, s is the width of the transmission lines feeding the patch elements as well as the separation between the transmission lines. For the FSS, p is the width of each square patch in the frequency selective surface, g is the gap between the square patches, and t is the total length of the surface.

The square patch antenna uses an edge feed, providing linear polarization to the antenna. Due to the symmetrical geometry of square patch antennas, one advantage provided decent cross-polarization, enabling increased reception of horizontally and vertically polarized linear waveforms incident upon the antenna. Within an energy harvesting application, this plays a significant role in increasing rectenna performance as a greater amount of ambient radio energy may be received and ultimately converted to usable DC voltage across the load resistance.

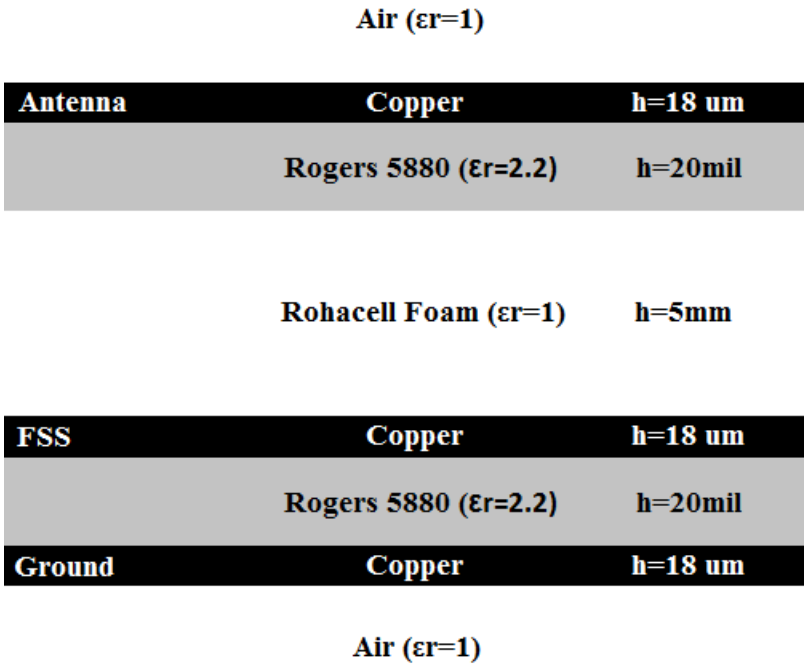

Figure 5.4: A layered diagram of the arrangement of materials used in the multi-layered antenna

5.2 Rectifier Circuitry

Significant energy scavenging using a rectenna for relatively low levels of ambient power density is very challenging. The key to low level energy recovery and efficiency is making certain that enough incident power is recovered so that the diodes operate in saturation for a significant portion of the cycle with very low loss(Vera, 2009). Therefore, selecting the correct RF diodes becomes very important. The MA4E1317 diodes were selected based on a comparison of the efficiency of several different diodes operating over the 2.4 - 2.5 GHz band ("MA4E1317 Datasheet"), (Vera, 2009).

The rectennas impedance matching network was connected to a balanced dual diode half-wave rectifier circuit as shown in (Ren and Chang, 2006). Two methods of rectification were considered using either a shunt diode or two series diodes. The measured output voltage

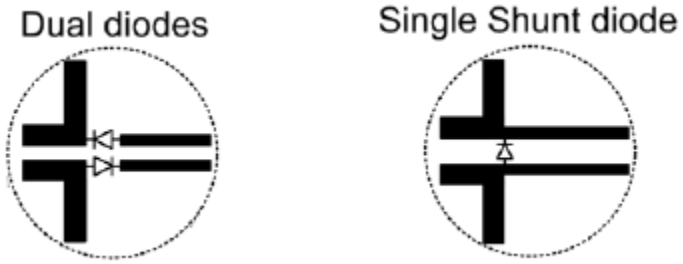

Figure 5.5: Single vs. Dual Diode Rectification (Ren and Chang, 2006)

and efficiency of the rectenna using a single shunt diode was significantly less than output voltage using two series diodes. A full-wave (4 diode) rectifier would be a likely extension of this work but was not considered here to reduce fabrication and balancing complexity (Ren and Chang, 2006).

Although the dual series diode rectification does not provide full-wave rectification, at 2.45 GHz the output voltage measured is nearly double that of the single-diode rectification with very little ripple voltage and was therefore selected for the design.

The diodes used have a zero-bias junction capacitance C_{j0}= .02 pF, a forward-bias turn on voltage V_{bi}= .7 V, and a variable series resistance $R_s = 4 \sim 7\ \Omega$ ("MA4E1317 Datasheet") dependent on the diode current. An additional 22 pF capacitor was added in shunt with the load as shown in Fig. 8.1 in order to mitigate ripple voltage. The use of the FSS allows for the antenna to be directly attached to the FSS in place of a lumped-element filter or stub matching network. The matching network was designed for optimal matching at 2.45 GHz however, due to the fabrication imperfections the measured efficiency was slightly less.

5.3 Simulation

The FSS is used in place of a traditional transmission line filtering system which typically consists of tuned shunt-stub transmission lines or tee resonators. The FSS used in this design consists of a periodic array of square patches with a separation between each patch. Capacitance is developed between adjacent conductive square patches across the gap

present between them. Therefore the widths of the square patches as well as the spacing between patches alter the level of capacitance present in the collective array. The widths of these square patches and the spacing between them have been swept using a parametric analysis to find the optimal capacitive tuning to best match the design frequency of the antenna (shown in figures 5.7 & 5.8). This serves as a matching network for the rectenna system while occupying the same area used by the ground plane.

Because the FSS was applied as a ground plane to the antenna, a square patch array was used due to both simplicity and increased reflection of the design.(Cure, Weller, and Miranda, 2013)

The mutual coupling present between the square patches in the periodic array along with the reflection of the square elements themselves allows the FSS to serve as a reflect array below the radiating antenna element. The sub-wavelength square patch elements present in the FSS behave as a quasi-static metamaterial surface, reducing the amount of radiation leaked through the FSS. Because radiations through the bottom surfaces of the rectenna are minimized and the back-lobing has been reduced, the usable to radiated emission from the top-side of the antenna is conserved.

In simulation, the FSS ground provides a more efficient cardioid-like radiation pattern to the rectenna (Fig. 5.6), allowing for a broad angle of reception for incident radio waves necessary in wireless scavenging applications.

5.4 Fabrication

5.4.1 Development

The first step in the fabrication process is to pattern the Rogers RT Duroid 5880 copper clad board.

Although many fabrication techniques involve the use of positively developed images, the Kepro bench-top developer utilizes a negative development technique and requires the transparency to be placed above the copper-side of the RT Duroid 5880 sample. The clear

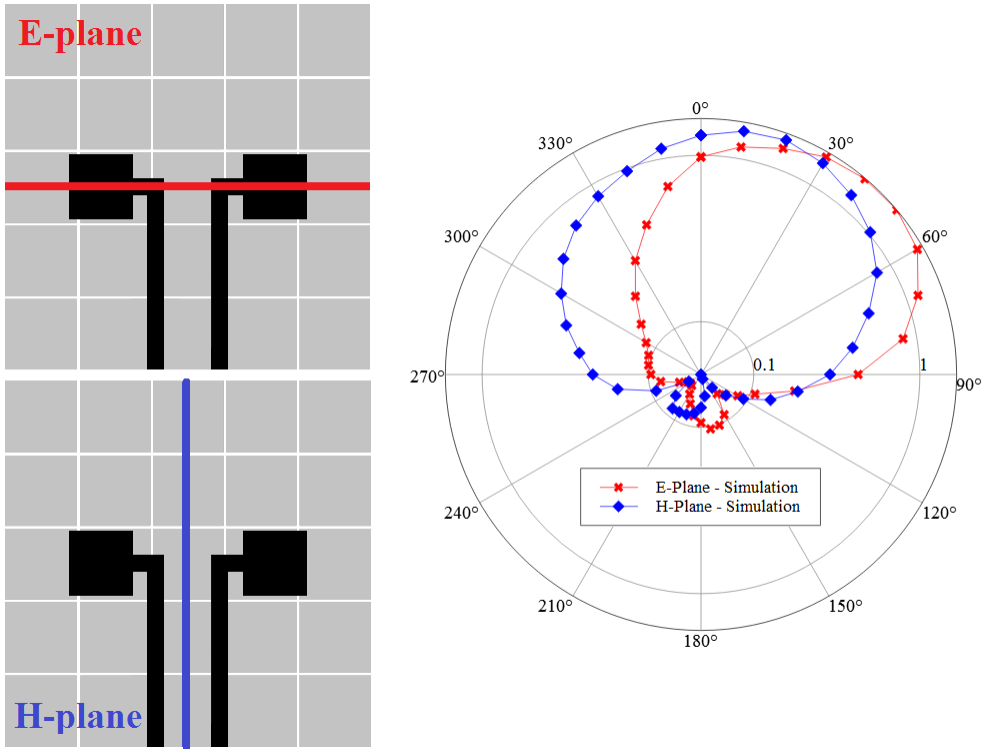

Figure 5.6: Simulated radiation patterns in the E-plane and H-plane of the FSS antenna

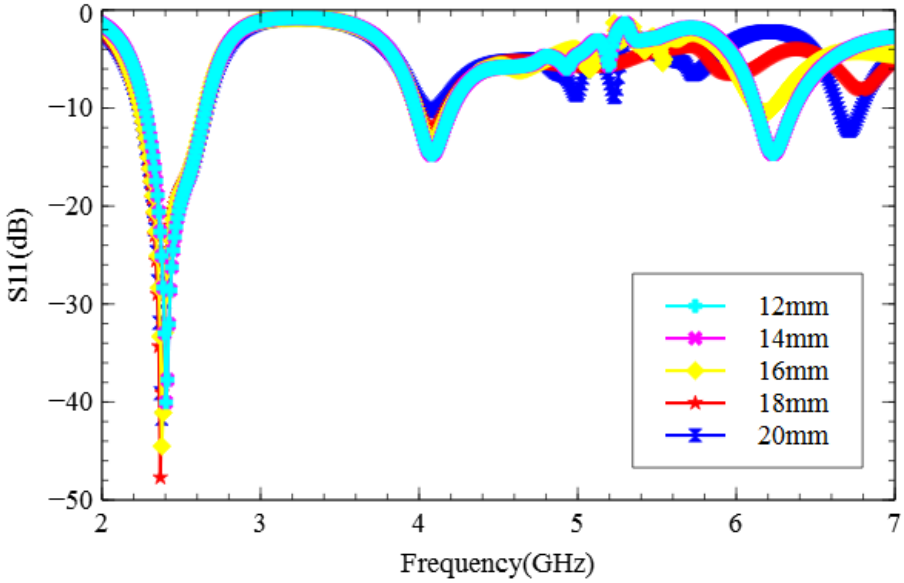

Figure 5.7: A parametric sweep of the patch widths used in the dipole antenna

regions of the transparency designate the regions of the PC board which retain copper cladding and the black regions indicate copper to be etched off the substrate.

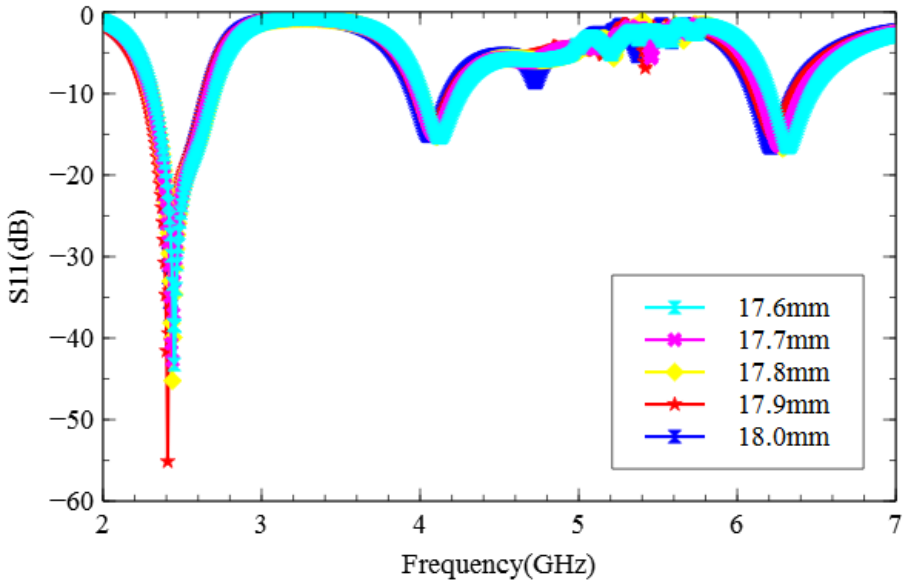

Figure 5.8: A parametric sweep of the patch widths used in the frequency selective surface

Figure 5.9: Kepro Bench-Top Developer

5.4.2 Etching

In order to remove the unwanted copper from the developed board, the exposed sample of RT Duroid 5880 is then placed in the Kepro etching machine. Areas not exposed to lighting in the stages of development are removed from the board using a laser etch technique.

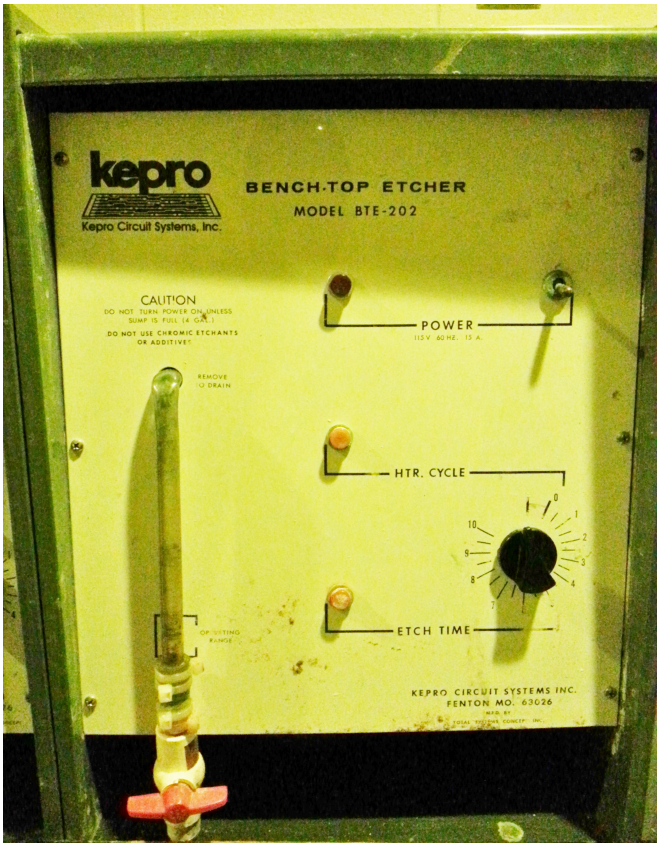

Figure 5.10: Kepro Bench-Top Etcher

5.4.3 Rinsing

After the board has been developed, unwanted chemical residue must be rinsed before being sent to the etcher. This rinse is done by the rinse unit shown in figure 5.11. Areas left with chemical residue may produce unwanted copper spots once etched. After etching, the board must once again go through an additional rinse cycle to remove the leftover residue left on the board from the etch cycle.

Figure 5.11: Kepro Bench-Top Rinser

5.4.4 Fabricated Antenna

Once the copper cladded board has been developed, rinsed and etched, the excess substrate is cut using a guillotine blade. This part of the fabrication process may take a toll on the performance of the structure as the guillotine is operated by hand and flaws in the symmetry of the antenna may appear due to human operation of the guillotine. Once cut to the desired dimensions, the board then had holes cut in the appropriate locations for the SMA end launch connector to be established. Once the connector was properly secured, the signal pin was soldered to the feed line of the antenna. The fully fabricated antenna design is shown in figure 8.1.

5.5 Measurement

A Keysight N9935A Vector Network Analyzer was used to measure the return loss of the rectenna. All radiation pattern measurements were performed in an anechoic chamber. The rectenna was placed in the boresight of a Scientific Atlantic standard gain horn antenna.

Attached using an SMA connection, the rectenna was measured on a rotating platform allowing for full E-plane and H-plane pattern measurements. Once measured data was relayed to the computer, Diamond Engineering's Antenna Measurement System (DAMS) was used to convert and plot the data.

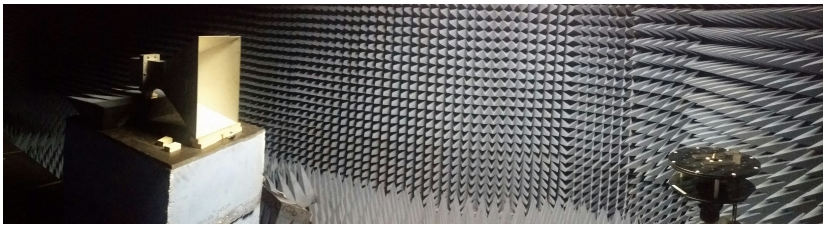

Figure 5.12: Panoramic side view of anechoic chamber

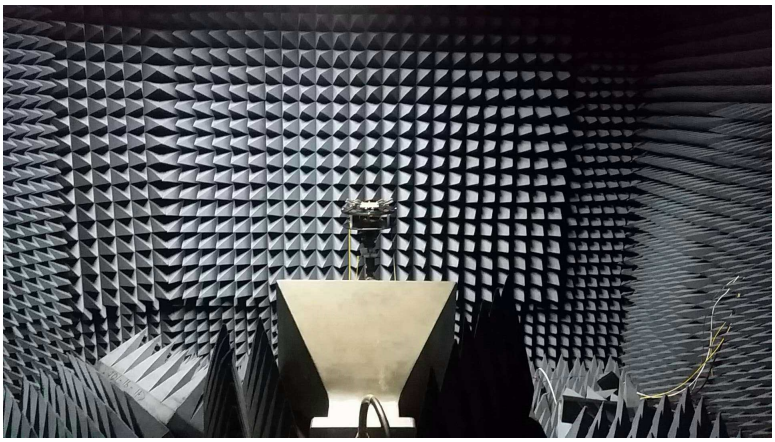

Figure 5.13: Boresight view of transmit antenna inside anechoic chamber

Chapter 6

Rectenna Theory

A rectenna system converts ambient radio energy to DC voltage; therefore, a primary figure of merit of rectenna systems is the RF-to-DC conversion efficiency. Because an antenna is used on the front-end of the rectenna system to receive incident radio energy, fundamental antenna theory and wave propagation equations are used to characterize the rectenna system.

The Friis transmission equation (eqn. 6.2) is used to evaluate the maximum possible power received at the antenna(P_r), assuming a free space environment. In this equation, the gain of the receive antenna (G_r)and gain of the transmit antenna (G_t) are included as well as the free space wavelength (λ_0) and the distance between transmit and receive antennas (R) (measurement setup shown in Fig. 7.1). Power density (P_{ave})(eqn. 6.3) is an important measure in rectenna applications as the DC output of the rectenna is contingent on the rectification of AC power available on the rectenna. This measure of power density places more emphasis on the conversion efficiency of the rectenna as opposed to an increase in output voltage.

The measured RF-to-DC conversion efficiency of the rectenna (eqn 6.4) is found by dividing the DC power across the load resistance by the receive power of the rectenna given by the Friis transmission equation. The DC power output by the rectenna is found by measuring the voltage and resistance across the load resistance using a digital multi-meter.

$$A_e = \frac{{\lambda_0}^2 G_r}{4\pi} \tag{6.1}$$

$$P_r = \frac{P_t A_e G_t}{4\pi R^2} \tag{6.2}$$

$$P_{ave} = \frac{P_t G_t}{4\pi R^2} \tag{6.3}$$

$$\eta = \frac{P_{DC}}{P_r} \cdot 100 \quad (\%) \tag{6.4}$$

To anticipate the performance of the rectification of the rectenna system, a closed-form approximation for nonlinear RF diode behavior from a previous work was used. (McSpadden, Fan, and Chang, 1998)

$$C_j = C_{Jo}\sqrt{\frac{V_{bi}}{V_{bi} + |V_o|}} \tag{6.5}$$

$$tan(\theta_{on}) - \theta_{on} = \frac{\pi R_s}{R_L(1 + \frac{V_{bi}}{V_o})} \tag{6.6}$$

$$A = \frac{R_L}{\pi R_s}(1 + \frac{V_{bi}}{V_o})^2[\theta_{on}(1 + \frac{1}{2cos^2(\theta_{on})}) - \frac{3}{2}tan(\theta_{on})] \tag{6.7}$$

$$B = \frac{R_s R_L C_j^2 \omega^2}{2\pi}(1 + \frac{V_{bi}}{V_o})(\frac{\pi - \theta_{on}}{cos^2(\theta_{on})} + tan(\theta_{on})) \tag{6.8}$$

$$C = \frac{R_L}{\pi R_s}(1 + \frac{V_{bi}}{V_o})\frac{V_{bi}}{V_o}(tan(\theta_{on}) - \theta_{on}) \tag{6.9}$$

$$\eta_{calc} = \frac{1}{1 + A + B + C} \tag{6.10}$$

Using component values from the data sheet of the L-band RF Schottky diodes used in the rectification circuit of the rectenna, the predicted RF-to-DC conversion efficiency (η_{calc}) is calculated using equation 6.10.(McSpadden, Fan, and Chang, 1998)

Where the electrical parameters used for the calculation include the diodes zero-bias junction capacitance (C_{jo}), the built-in voltage of the diode in the forward-bias region (V_{bi}), the output self-bias DC voltage (V_o), the nonlinear junction capacitance (C_j), diode series resistance (R_s), DC load resistance (R_L), a dynamic variable dependent on the forward-bias turn-on angle (θ_{on}), and angular frequency (w).

Chapter 7

Experiment

The experimental configuration adopted from a previous study was setup so that the parameters required for equations 6.1-6.4 were observable (McSpadden, Fan, and Chang, 1998). Providing a far-field analysis of the rectenna, this allowed for RF wireless transmission efficiency to be observed as opposed to near-field induction and coupling . Because there is a separation of only 2m between a 2.45 GHz transmitter and receiver, near field effects may effect the received power in this experiment.

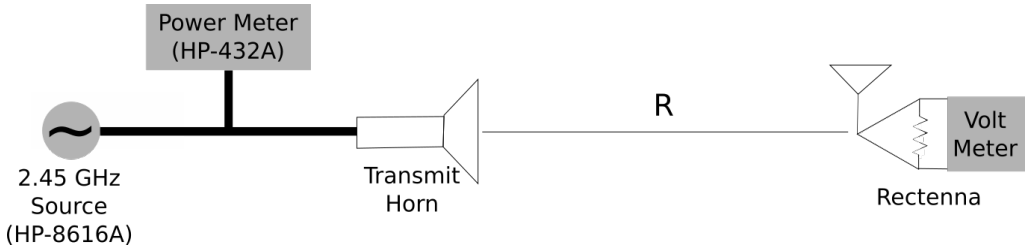

Figure 7.1: Experimental Setup for Rectenna Measurement

A frequency synthesizer provides a 2.45 GHz pulse fed through a power amplifier. The power of the amplified RF signal is then connected to a power meter and standard gain horn antenna. The rectenna is placed in the boresight of the transmitting horn 2m away. The incident power at the rectenna is received and converted to DC. Finally, the DC voltage is measured across the load resistance of the rectenna using a multi-meter. Once the voltage across the known load resistance is measured, Ohms law is used to calculate the DC power output from the rectenna.

Using this experimental setup, the performance of two variations of the proposed rectenna was measured. In each of the variations, the rectification circuit is altered while the rest of the rectenna does not vary.

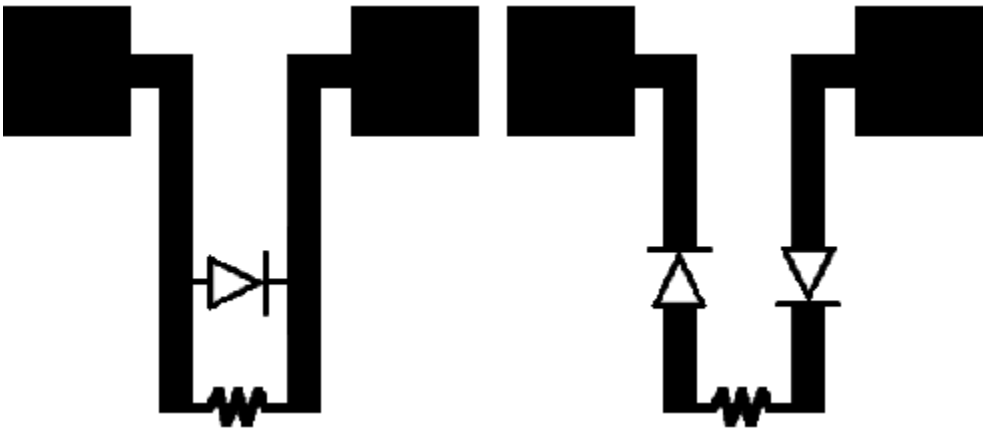

Figure 7.2: Single-diode shunt configuration of rectenna (left), Dual-diode series configuration of rectenna (right)

The first rectification method tested uses a single diode placed in parallel between the two transmission lines extending from the antenna. This is the more traditional rectification method seen among rectenna systems. The second rectification method tested uses two diodes places in series within each of the transmission lines prior to termination across the load resistance. This rectification method was introduced in a reviewed work (Ren and Chang, 2006) and is proven to achieve higher AC-to-DC conversion efficiencies within RF frequencies. The validity of both rectification configurations for this rectenna design is evaluated.

Chapter 8

Results

The rectenna was designed to operate at a center frequency of 2.45 GHz and has a -10 dB S_{11} bandwidth from 2.44 GHz to 2.62 GHz with a minimum return loss of -42.12 dB at 2.485 GHz (shown in Fig. 8.2). This frequency range was chosen due to the significant amount of ambient microwave energy radiated in the 2.4 GHz - 2.5 GHz ISM band Donchev et al., 2014.

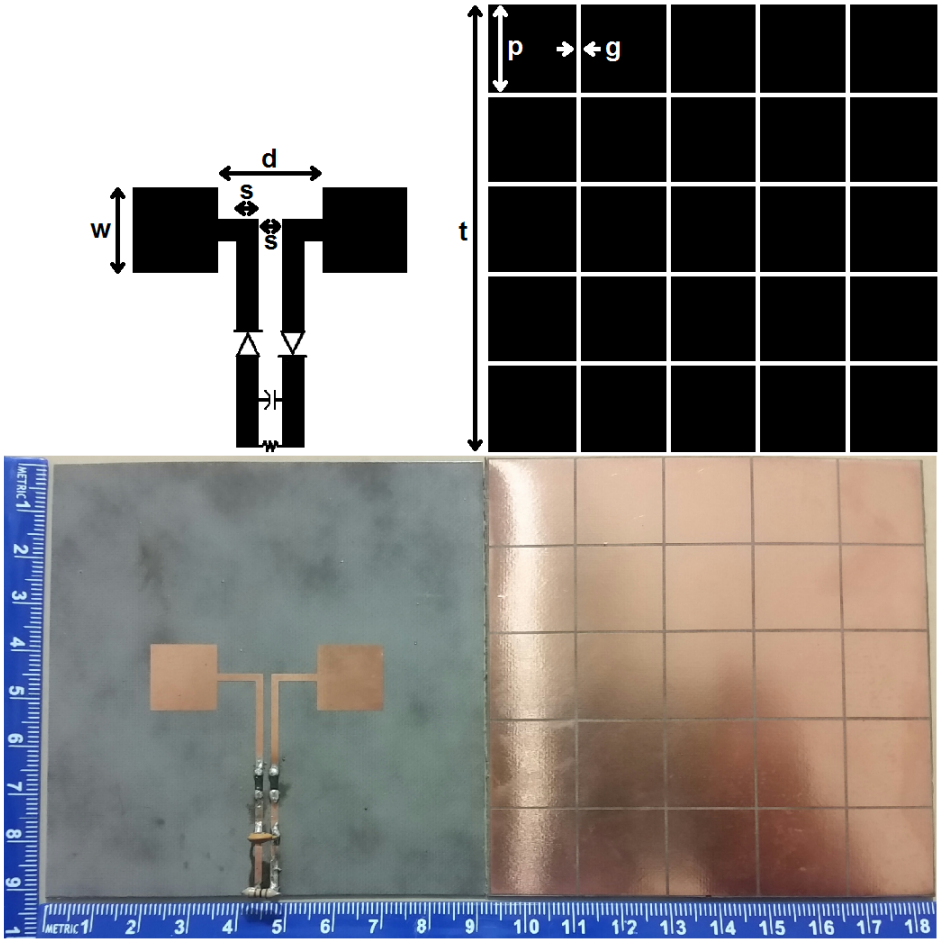

Figure 8.1: Dimensions of fabricated FSS Rectenna

Table 8.1: Dimensions of FSS Rectenna

w	d	s	p	g	t
16 mm	20.8 mm	1.6 mm	17.9 mm	.5 mm	92 mm

The exact dimensions of the FSS patch size and spacing were determined using the optimization toolkit's parametric sweep feature of HFSS (Fig. 5.8) and found to be 17.9 mm x 17.9 mm with a separation of g = 0.5 mm. The antenna patch size was 16 mm x 16 mm with a peak directivity of 6.15 dB at 2.5 GHz.

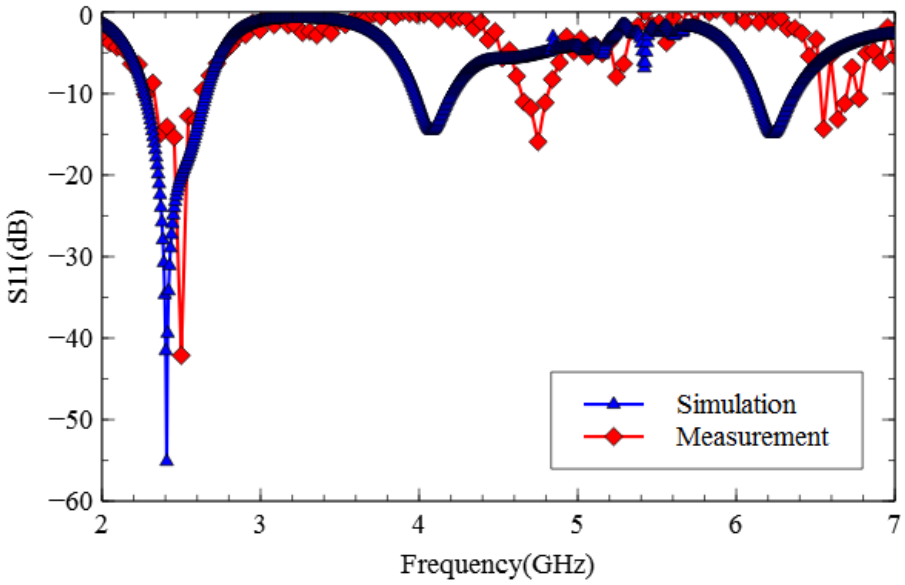

Figure 8.2: Return loss of antenna simulation and measurement

Because the FSS was applied as a ground plane to the antenna, a square patch array was used due to both simplicity and increased reflection of the design.(Cure, Weller, and Miranda, 2013)

The mutual coupling between the periodic array of square patches helps impedance match the overall structure and also provides a strong reflection. This allows the FSS to serve as a reflect array below the radiating antenna element. Because radiations through the bottom surfaces of the rectenna are minimized and the back-lobing has been reduced, the usable to radiated emission from the top-side of the antenna is conserved.

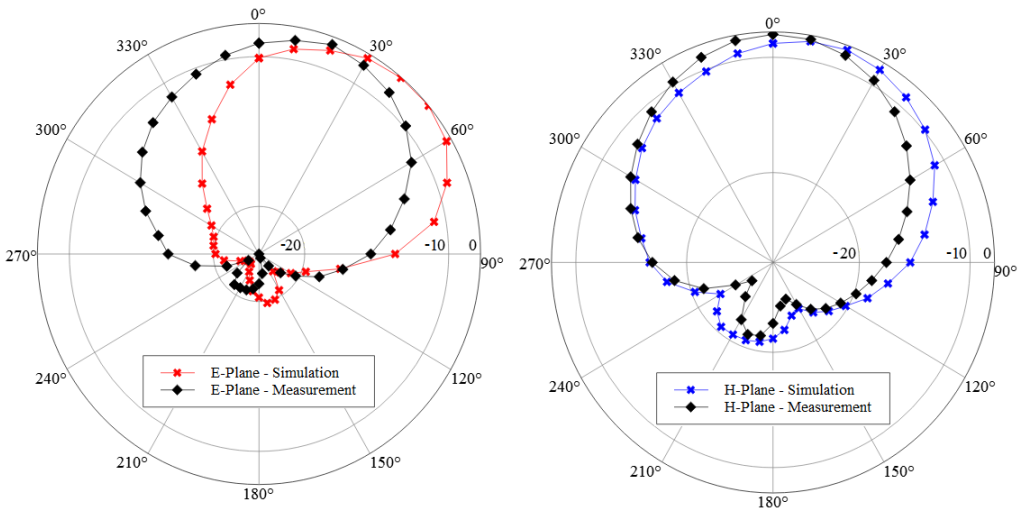

Figure 8.3: Simulated and measured radiation patterns in the E-plane and H-plane of the FSS antenna

This provided a relatively broad angle of incident energy reception. The simulated E plane power pattern was in good agreement with the E plane measurement and shown in Fig. 8.3. The simulated E and H plane power patterns are very similar and a comparison of the E and H plane simulated power patterns to measurements is shown in Fig. 8.3.

For the rectenna design presented, the output voltages for the traditional single diode in parallel rectification circuit is measured and compared to the newer dual-series diode rectification method. Both rectification methods are measured at equal power densities over various load resistances. Viewing the measurement results, it is observed that the dual-series diode rectification yields a significantly higher output voltage when compared to the single-shunt diode rectification over the same range of power density incident upon the rectenna. Due to the favorable performance demonstrated in output voltage, the dual series diode rectification approach was adopted for the final rectenna design.

Although a main purpose of a rectenna is to convert incident RF energy upon the rectenna to DC voltage, how efficiently this RFto-DC conversion is achieved is a key figure of merit in valuing rectenna performance. Due to enhanced AC-to-DC conversion attributed to the dual-diode rectification in addition to minimized return loss of the aggregate RF

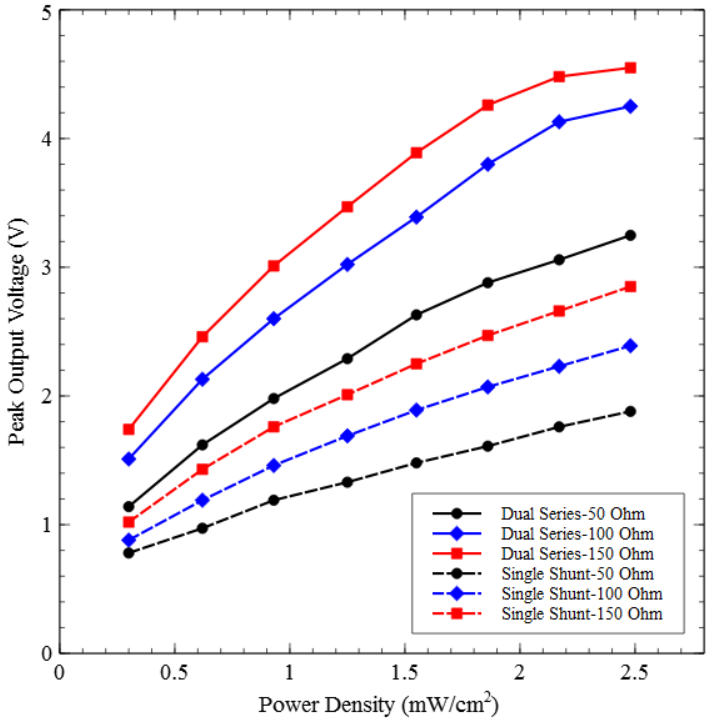

Figure 8.4: Output voltage measurements for rectenna using single shunt diode and dual series diode configurations over multiple load resistances

structure, decent conversion efficiency is demonstrated at the operating frequency of 2.45 GHz.

Another trend that was observed is that increasing the load resistance increased the output voltage/power for a limited range of input power densities. However, it should be noted that an increased load voltage does not indicate increased efficiency or output power which are limited by the antenna's radiation resistance and aperture. The measured RF-to-DC conversion efficiency shows good agreement when compared to the predicted efficiencies given by Eq. 6.9 and the comparison shown in Fig. 8.5. The slight differences observed between measurements and calculations can be attributed to fabrication errors and uncertainties in antenna alignment. The optimal conversion efficiency of 79% was achieved using a 100 Ω load resistance and is shown in Fig. 8.5.

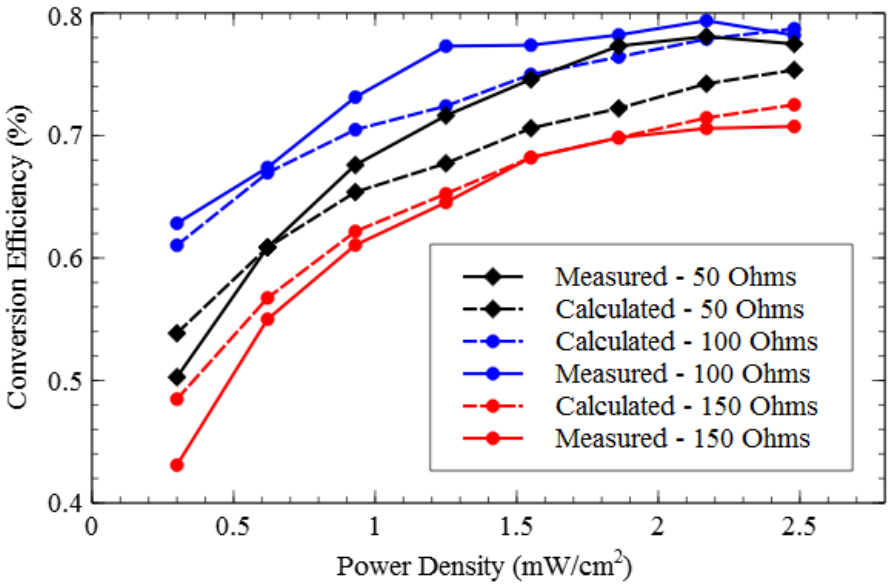

Figure 8.5: Calculated and measured conversion efficiencies for the rectenna over multiple load resistances

Chapter 9

Conclusion

In this research, a rectenna design based on a dual patch antenna using dual-diode rectification was presented. The novelty of this design is the use of a FSS for impedance matching instead of the commonly used stub matching circuits.

The 79% conversion efficiency of the FSS dual diode system was 3% greater than the dual-diode stub matched system shown in (Ren and Chang, 2006). A comparison of measured and estimated conversion efficiencies versus incident power density is shown in Fig. 8.5 and in all cases the overall agreement was excellent.

A comparison of the FSS sqaure patch rectenna to other state-of-the-art shunt stub matched rectenna designs is provided in Table 9.1.

Table 9.1: Comparison of matching, RF-to-DC conversion efficiency, output voltage and size of shunt-stub matched rectennas to FSS rectenna

	S_{11}	η	V_0	Antenna Length
Square Patch (Ren and Chang, 2006)	-22 dB	76%	6.22 V	1.35λ
Monopole T-line (Lee and Chang, 2015)	-30 dB	66%	2.6 V	1.2λ
Broadband Printed (Hong et al., 2010)	-40 dB	81%	1.98 V	4.89λ
FSS Square Patch	-43 dB	79%	4.13 V	0.591λ

The rectenna design had a provided a broad angle for incident energy reception with E-plane and H-plane beamwidths of ($\theta_{E_{3dB}} = 87°$,$\phi_{H_{3dB}} = 82°$) respectively with a maximum directivity of 6.15 dBi.

The use of the FSS in place of a usual stub matching network reduces the surface area of the rectenna while also providing improved matching. This improved matching and reduction in return loss allows for the overall RF-to-DC conversion to be achieved more efficiently. The

maximum measured RF-to-DC conversion efficiency was found to be 79% for a 100 Ω load resistance with a maximum output voltage at 4.13 V.

The overall performance of the FSS rectenna design was very good, suggesting it could be used in place of the traditional stub matching designs for energy harvesting.

Bibliography

Bouwman, Ronald (2008). "The Amplitron, aka Cross-Field Amplifier". In: *Radar Systems for Technicians*.

Brown, Aneline (2010). "RFID, the "Killer Rabbit"?" In:

Brown, WC and JF Triner (1982). "Experimental thin-film, etched-circuit rectenna". In: *1982 IEEE MTT-S International Microwave Symposium Digest*, pp. 185–187.

Cure, D, T Weller, and F Miranda (2011). "A comparison between Jerusalem Cross and Square Patch Frequency Selective Surfaces for low profile antenna applications". In: pp. 1019–1022.

Cure, David, Thomas M Weller, and Félix A Miranda (2013). "Study of a low-profile 2.4-GHz planar dipole antenna using a high-impedance surface with 1-D varactor tuning". In: *Antennas and Propagation, IEEE Transactions on* 61.2, pp. 506–515.

Donchev, Evgeniy et al. (2014). "The rectenna device: From theory to practice (a review)". In: *MRS Energy & Sustainability* 1, E1.

Electronics360 (2015). *Intel Helps with Honey Bee Health Tracking*.

Farandos, Nicholas M et al. (2015). "Contact lens sensors in ocular diagnostics". In: *Advanced healthcare materials* 4.6, pp. 792–810.

Hong, Tae-Ui et al. (2010). "Novel broadband rectenna using printed monopole antenna and harmonic-suppressed stub filter". In: *Microwave and Optical Technology Letters* 52.5, pp. 1194–1197.

Hooberman, Benjamin (2005). "Everything you ever wanted to know about frequency-selective surface filters but were afraid to ask". In: *New York (NY): Technical Report, Department of Physics, Columbia University*.

Inc., ANSYS. "High Frequency Structural Simulator v15". In:

Lee, Chien-Hsing and Yu-Han Chang (2015). "Design of a broadband circularly polarized rectenna for microwave power transmission". In: *Microwave and Optical Technology Letters* 57.3, pp. 702–706.

M/A-COM Technology Solutions, Inc. "MA4E1317 Datasheet". In:

Mannoor, Manu S et al. (2012). "Graphene-based wireless bacteria detection on tooth enamel". In: *Nature communications* 3, p. 763.

McSpadden, James O, Lu Fan, and Kai Chang (1998). "Design and experiments of a high-conversion-efficiency 5.8-GHz rectenna". In: *Microwave Theory and Techniques, IEEE Transactions on* 46.12, pp. 2053–2060.

MHS (2008). *William C. Brown*.

Mitani, Tomohiko et al. (2006). "Study on High-Efficiency and Low-Noise Wireless Power Transmission for Solar Power Station/Satellite". In: *Presentation at the Sustainable Energy and the Environment Conference (SEE2006)*.

Morelle, Rebecca (2008). "Tiny tags track brainy bumblebees". In:

New York, Tesla Memorial Society of (1904). *New York American - Tesla's Tower*.

Peixeiro, Custódio (2011). "Microstrip patch antennas: An historical perspective of the development". In: *Microwave & Optoelectronics Conference (IMOC), 2011 SBMO/IEEE MTT-S International*. IEEE, pp. 684–688.

Ren, Yu-Jiun and Kai Chang (2006). "5.8-GHz circularly polarized dual-diode rectenna and rectenna array for microwave power transmission". In: *Microwave Theory and Techniques, IEEE Transactions on* 54.4, pp. 1495–1502.

Sothcott, Simon (2011). *What is RFID? - 10 Examples of RFID Applications*.

Systems, Checkpoint. "4210 EP Food Label". In:

Vera, G Andia (2009). "Efficient Rectenna Design for Ambient Microwave Energy Recycling". In: *Bachelor Degree Philosophy, Univerat Politecnica de Catalunya*.

Wilson, Tracy (2015). *How Wireless Power Works*.

Wu, Kaijie, Debaditya Choudhury, and Hirokazu Matsumoto (2013). "Wireless power transmission, technology, and applications [Scanning the issue]". In: *Proceedings of the IEEE* 101.6, pp. 1271–1275.

Yuwei, Zou et al. (2010). "Current research situation and developing tendency about wireless power transmission". In: *Electrical and Control Engineering (ICECE), 2010 International Conference on*. IEEE, pp. 3507–3511.

Appendix A

Materials Used

Figure A.1: Rogers 5880 Duroid Substrate

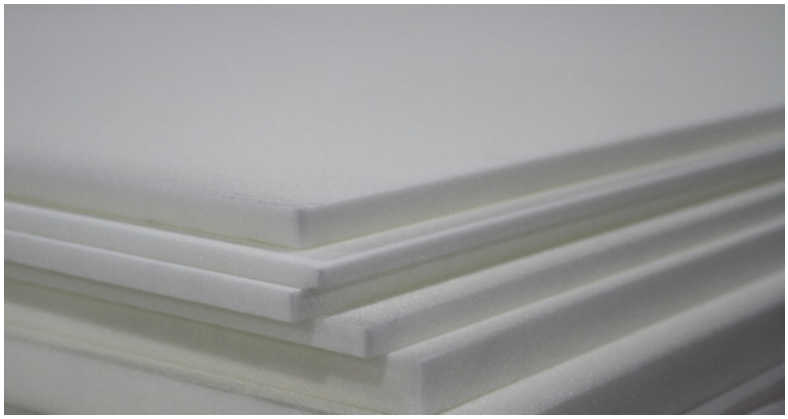

Figure A.2: Rohacell HF 71 Foam

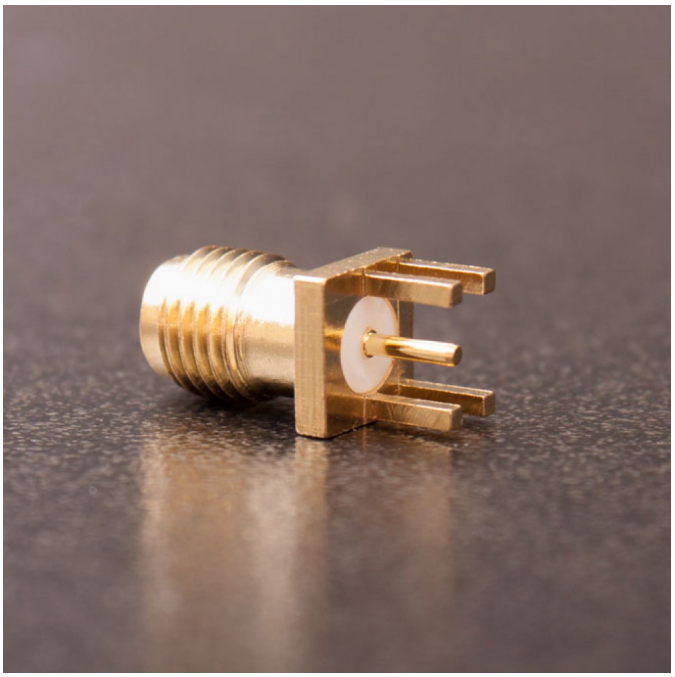

Figure A.3: SMA End Launch PCB Connector

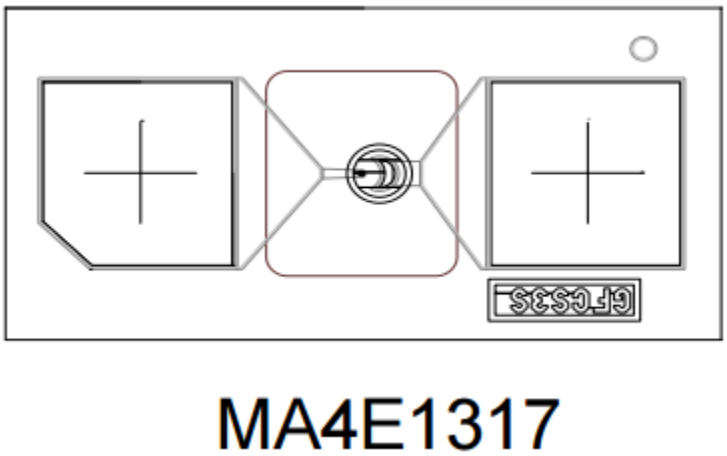

Figure A.4: MA4E1317 RF Schottky Diode

Appendix B

Measurement Instruments

Figure B.1: Keysight 9335A Network Analyzer

Figure B.2: HP-8616A Frequency Generator

Figure B.3: HP-432A Power Meter